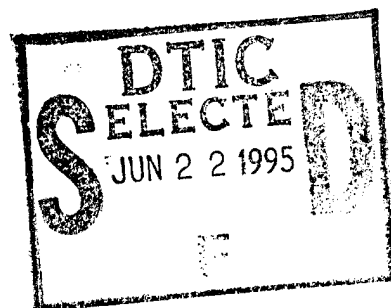




National  
Defence

Défense  
nationale



# **ANALYSIS AND OPTIMIZATION OF THE DATA COLLECTION PROCESS OF TIME-INTEGRATING CORRELATORS**

by

**N. Brousseau and J.W.A. Salt**

This document has been approved  
for public release and sale; its  
distribution is unlimited.

DTIC QUALITY INSPECTED 8

**DEFENCE RESEARCH ESTABLISHMENT OTTAWA**  
TECHNICAL NOTE 95-5

**Canada**

March 1995  
Ottawa

**19950620 067**



National    Défense  
Defence    nationale

# ANALYSIS AND OPTIMIZATION OF THE DATA COLLECTION PROCESS OF TIME-INTEGRATING CORRELATORS

by

**N. Brousseau and J.W.A. Salt**  
*Electronic Support Measures Section*  
*Electronic Warfare Division*

Accession For	
NTIS CRA&I	<input checked="checked" type="checkbox"/>
DTIC TAB	<input type="checkbox"/>
Unannounced	<input type="checkbox"/>
Justification	
By	
Distribution /	
Availability Codes	
Dist	Avail and/or Special
A-1	

**DEFENCE RESEARCH ESTABLISHMENT OTTAWA**  
TECHNICAL NOTE 95-5

PCN  
041LY

March 1995  
Ottawa

## ABSTRACT

The features of the detection process of a TIC have been studied with a computer simulation. Optimal conditions of operation, allowing a reliable detection of the correlation peaks over the whole operating window, have been established. These optimal conditions have the advantage to allow a graceful degradation of the detection process performances when the parameters drift away from their optimal value. Of particular importance is the fact that the detection process is not sensitive to large change of temperature when an optimal modulation is used. It is also demonstrated that the exact shape of the sensitivity response of the detector array element is a parameter of secondary importance in the evaluation of the detection process performance. Experimental verifications of the optimal detection process has confirmed its capability to detect reliably correlation peaks over the whole field of view of the TIC.

## RESUME

On étudie les caractéristiques du processus de détection d'un corrélateur à intégration temporelle (CIT) à l'aide d'une simulation par ordinateur et on détermine les conditions d'opération optimales pour la détection fiable de pics de corrélation sur toute la fenêtre d'opération. Ces conditions d'opération optimales ont l'avantage supplémentaire d'être associées à une détérioration progressive des performances du processus de détection si les paramètres d'opération s'écartent un peu des valeurs optimales. Il est particulièrement important de noter que le processus de détection est indépendant des changements de température lorsqu'un système de franges optimal est utilisé. Il est aussi démontré que la forme particulière du profil de sensibilité des éléments du photodétecteur est un paramètre d'importance secondaire dans la performance du système. Des vérifications expérimentales du processus de détection optimal ont confirmé sa capacité à détecter de façon fiable des pics de corrélation sur tout le champ d'opération du CIT.

## EXECUTIVE SUMMARY

Time-Integrating Correlators can be used to compare signals. The decisions on the identity or similarity of the signals are based on the amplitude of the correlation peaks produced by the TIC. It is consequently very important to understand and control the impact of the data collection process on the measured intensity of the peaks.

This technical note contains an analysis and an optimization of the data collection process of a TIC where factors such as the format of the light distribution produced by the correlator and the size, position and sensitivity response of the elements of the detector array are taken into consideration. The features of the detection process of a TIC have been studied with a computer simulation and optimal conditions of operation allowing a reliable detection of the correlation peaks over the whole operating window have been established. These optimal conditions of operation have the further advantage to be associated with a graceful degradation of the performances of the detection process if the parameters drift away from their optimal value. Of particular importance is the fact that the detection process is not sensitive to large change of temperature when an optimal modulation is used. Experimental verifications of the optimal detection process has confirmed their capability to detect reliably correlation peaks over the whole field of view of the TIC.

## TABLE OF CONTENTS

	<u>PAGE</u>
ABSTRACT/RESUME	iii
EXECUTIVE SUMMARY	v
TABLE OF CONTENTS	vii
LIST OF FIGURES	
LIST OF ABBREVIATIONS	
 1.0 INTRODUCTION	 1
2.0 DESCRIPTION OF A TIME-INTEGRATING CORRELATOR	1
3.0 DESCRIPTION OF THE SIMULATION	5
3.1 Format of the Light Distribution	5
3.2 Detection Process	7
3.3 Description of the Main Programs	7
4.0 FEATURES OF THE DETECTION PROCESS	11
4.1 Effects of the Location of the Detecting Elements	14
4.2 Effects of the Phase Difference Between the RF Input Signals	14
5.0 OPTIMAL DETECTION PARAMETERS	20
5.1 For a Uniform Sensitivity Response	20
5.2 For the Sensitivity Response of the Thompson CSF Detector	26
6.0 EXPERIMENTAL VERIFICATIONS	27
7.0 CONCLUSION	31
8.0 REFERENCES	34
APPENDIX A DECONVOLUTION OF THE EXPERIMENTAL MEASUREMENT OF THE SENSITIVITY RESPONSE OF A DETECTOR ARRAY	35

# LIST OF FIGURES

	<u>PAGE</u>
FIGURE 1: TIME-INTEGRATING CORRELATOR: TANDEM ARCHITECTURE.	2
FIGURE 2: CORRELATION PEAKS ON A PEDESTAL: A) NO MODULATION B) WITH MODULATION	4
FIGURE 3: A) THE MEASURED SENSITIVITY PROFILE FROM THE THOMPSON CSF TH 7805 DETECTOR ARRAYS, B) THE DIFFRACTION PATTERN THAT WAS USED TO SCAN THE ARRAY C) AND THE DECONVOLVED SENSITIVITY PROFILE	6
FIGURE 4: DEFINITION OF THE INPUT PARAMETERS FOR THE COMPUTER SIMULATION WHERE W IS THE WIDTH OF THE BASE OF THE TRIANGULAR ENVELOPE.	9
FIGURE 5: EXAMPLE OF THE OUTPUT FROM PUBDET WITH W=12, P=10, C=25 AND $\phi=\pi/2$ FOR A RECTANGULAR SENSITIVITY RESPONSE OF THE DETECTOR.	10
FIGURE 6: EXAMPLE OF THE OUTPUT FROM DIESEL WITH W=12 AND P=10 FOR A RECTANGULAR SENSITIVITY RESPONSE OF THE DETECTOR.	12
FIGURE 7: OUTPUT FROM A TIME-INTEGRATING CORRELATOR WITH MODULATION FOR W=6, C=25 AND $\phi=0$ AND $\pi/2$ FOR A RECTANGULAR SENSITIVITY RESPONSE OF THE DETECTOR.	13
FIGURE 8: OUTPUT FROM A TIME-INTEGRATING CORRELATOR FOR W=4, C=25, P=500 AND $\phi=0$ AND $\pi/2$ FOR A RECTANGULAR SENSITIVITY RESPONSE OF THE DETECTOR.	15
FIGURE 9: OUTPUT FROM A TIME-INTEGRATING CORRELATOR FOR W=4, P=500, $\phi=0$ AND C=0, 10, 20, 30, 40 AND 50 FOR A RECTANGULAR SENSITIVITY RESPONSE OF THE DETECTOR.	16
FIGURE 10: AMPLITUDE OF THE PEAK AS A FUNCTION OF THE POSITION OF THE APEX OF THE TRIANGULAR ENVELOPE ON THE DETECTING ELEMENT WITH A VERY LARGE MODULATION PERIOD FOR W=4, P=500, $\phi=0$ , FOR A RECTANGULAR SENSITIVITY RESPONSE OF THE DETECTOR.	17

# LIST OF FIGURES (cont'd)

	<u>PAGE</u>
FIGURE 11: OUTPUT FROM A TIME-INTEGRATING CORRELATOR FOR $W=10$ , $P=500$ , $\phi=0$ AND $C=0, 10, 20, 30, 40$ AND $50$ FOR A RECTANGULAR SENSITIVITY RESPONSE OF THE DETECTOR.	18
FIGURE 12: AMPLITUDE OF THE PEAK AS A FUNCTION OF THE POSITION OF THE APEX OF THE TRIANGULAR ENVELOPE ON THE DETECTING ELEMENT: WITH A VERY LARGE MODULATION PERIOD FOR $W=10$ , $P=500$ , $\phi=0$ FOR A RECTANGULAR SENSITIVITY RESPONSE OF THE DETECTOR.	19
FIGURE 13: OUTPUT FROM A TIME-INTEGRATING CORRELATOR FOR A RECTANGULAR SENSITIVITY RESPONSE OF THE DETECTOR AND WITH A) $W=10$ , $C=25$ , $P=20$ AND $\phi=0$ . B) $W=10$ , $C=25$ , $P=20$ AND $\phi=\pi/2$ . C) AMPLITUDE OF THE PEAK AS A FUNCTION OF THE POSITION OF THE APEX OF THE TRIANGULAR ENVELOPE ON THE DETECTING ELEMENT: THE MODULATION PERIOD IS VERY LARGE AND $W=10$ , $P=5000$ , $C=0$ AND $\phi=\pi/2$ .	21
FIGURE 14: AMPLITUDE OF THE PEAK AS A FUNCTION OF THE POSITION OF THE APEX OF THE TRIANGULAR ENVELOPE ON THE DETECTING ELEMENT FOR $W=6$ AND $P=4, 5, 6$ AND $7$ FOR A RECTANGULAR SENSITIVITY RESPONSE.	22
FIGURE 15: AMPLITUDE OF THE PEAK AS A FUNCTION OF THE POSITION OF THE APEX OF THE TRIANGULAR ENVELOPE ON THE DETECTING ELEMENT FOR $W=8$ AND $P=5, 6, 7$ AND $8$ FOR A RECTANGULAR SENSITIVITY RESPONSE.	23
FIGURE 16: AMPLITUDE OF THE PEAK AS A FUNCTION OF THE POSITION OF THE APEX OF THE TRIANGULAR ENVELOPE ON THE DETECTING ELEMENT FOR $W=10$ AND $P=5, 6, 7$ AND $8$ FOR A RECTANGULAR SENSITIVITY RESPONSE.	24
FIGURE 17: AMPLITUDE OF THE PEAK AS A FUNCTION OF THE POSITION OF THE APEX OF THE TRIANGULAR ENVELOPE ON THE DETECTING ELEMENT FOR $W=12$ AND $P=5, 6, 7$ AND $8$ FOR A RECTANGULAR SENSITIVITY RESPONSE.	25

LIST OF FIGURES (cont'd)

	<u>PAGE</u>
FIGURE 18: AMPLITUDE OF THE PEAK AS A FUNCTION OF THE POSITION OF THE APEX OF THE TRIANGULAR ENVELOPE ON THE DETECTING ELEMENT FOR $W=6$ AND $P=4, 5, 6$ AND $7$ FOR A THOMPSON CSF DETECTOR ARRAY WITH THE SAME ILLUMINATION LEVEL THAN THE RECTANGULAR SENSITIVITY RESPONSE.	28
FIGURE 19: AMPLITUDE OF THE PEAK AS A FUNCTION OF THE POSITION OF THE APEX OF THE TRIANGULAR ENVELOPE ON THE DETECTING ELEMENT FOR $W=6$ AND $P=4, 5, 6$ AND $7$ FOR A THOMPSON CSF DETECTOR ARRAY WITH THE ILLUMINATION LEVEL INCREASED BY A FACTOR OF $1.2$ .	29
FIGURE 20: THE SIX AUTO CORRELATION PEAKS THAT APPEARS IN THE TIC WINDOW WHEN THE CHIP RATE IS $20$ MHZ.	30
FIGURE 21: AMPLITUDE OF THE CORRELATION PEAKS OF FIGURE 20 AS A FUNCTION OF THE PHASE OF THE RF SIGNAL TO ONE BRAGG CELL.	32
FIGURE 22: CORRELATION PEAKS PRODUCED BY A $7$ -CHIP LONG CODE AND A CHIP RATE OF $10$ MHZ.	33



## 1.0 INTRODUCTION

Time-Integrating Correlators (TIC)s are analog optical computers designed to correlate two data streams of long duration. The two input Radio Frequency (RF) signals to process are introduced in the optical system via acousto-optic interaction in Bragg cells. The correlation is produced when the images of the two light distributions in the Bragg cells are coherently added and time-integrated by a linear detector array.

TICs can be used to compare signals in applications such as DNA analysis[1], code division multiple access communications and search of large databases of various kinds. The subsequent decisions on the identity or similarity of the signals are based on the amplitude of the correlation peaks produced by the TIC. It is consequently very important to understand and control the impact of the data collection process on the measured intensity of the peaks.

This technical note contains an analysis and an optimization of the data collection process of a TIC where factors such as the format of the light distribution produced by the correlator and the size, position and sensitivity response of the elements of the detector array are taken into consideration. The ideal case of collecting the data from a detector with a uniform sensitivity response is analysed by a simulation. The more realistic situations where a Thompson CSF THX 1061 board and a Thompson CSF TH7805 detector array detector are used is also analysed by the simulation and optimal conditions of operation are determined for each case. Experimental results are presented to validate the results of the simulation.

## 2.0 DESCRIPTION OF A TIME-INTEGRATING CORRELATOR

The techniques used to construct optical TIC are well documented in the literature [2-6]. We have chosen to illustrate the concept of TICs by using a tandem architecture described in [6] (Figure 1). The correlation between two signals  $a(t)$  and  $b(t)$  is mathematically described by:

$$f(t) = \int_0^U a(u) b(t-u) du$$

In an optical TIC, each of the two signals  $a(t)$  and  $b(t)$  is first applied to one Bragg cell. The Bragg cells are oriented in opposite directions (Figure 1). The signals are thus propagating in opposite directions, a condition needed for correlation. A computer generated hologram divides the laser beam into two beams

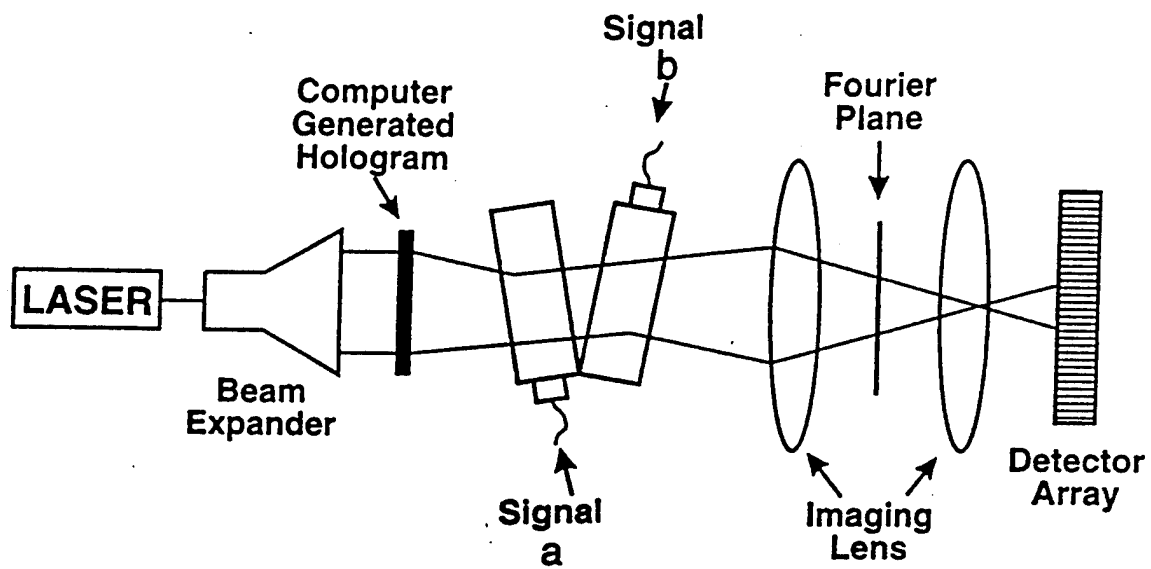


FIGURE 1: TIME-INTEGRATING CORRELATOR: TANDEM ARCHITECTURE

propagating at an angle such that each beam interacts with only one of the Bragg cells. The information contained in each RF signal is simultaneously transferred to the optical beams illuminating the Bragg cells. The optical signals diffracted by the Bragg cells now contain the information of the two RF signals. If the variable  $z$  is the distance along the Bragg cells and their images, and if the origin  $z=0$  is defined to be at the centre of their images on the detector array, the optical signals diffracted by the Bragg cells are  $a(t+z/v)$  and  $b(t-z/v)$ .  $v$  is the velocity of propagation of the signals in the Bragg cells. These light distributions are imaged on a linear array of photodetector by a series of lenses and spatial filtering. The detected electrical signal  $S(t,z)$  is proportional to the square of the light distribution.

$$s(t,z) = |a(t+z/v) + b(t-z/v)|^2$$

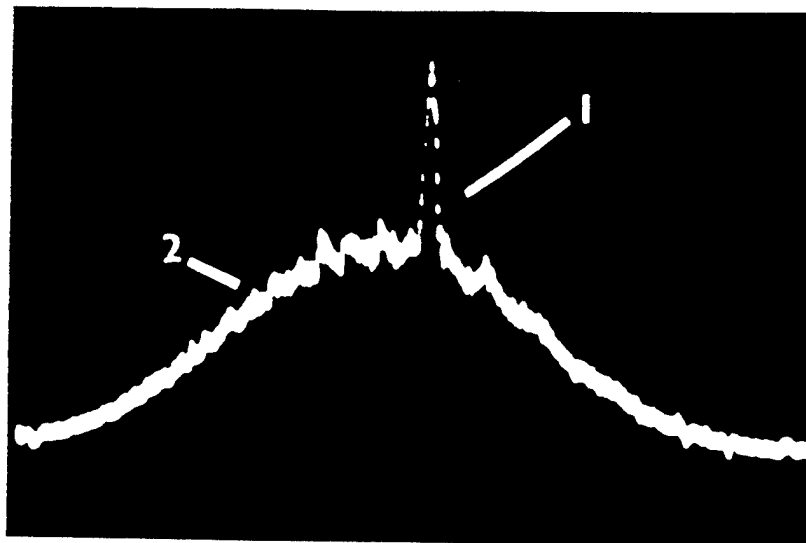
$$s(t,z) = a^2(t+z/v) + b^2(t-z/v) + a(t+z/v)b^*(t-z/v)$$

This electrical signal is then time-integrated by the elements of the detector array and the resulting signal  $S(T,z)$  is:

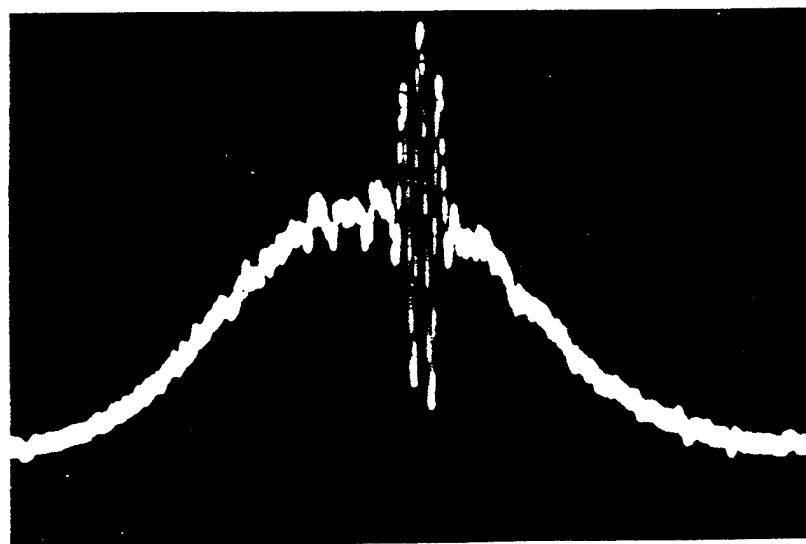
$$S(T,z) = \int_0^U [a^2(t+z/v) + b^2(t-z/v) + a(t+z/v)b^*(t-z/v)] dt$$

The first two terms give an undesired pedestal and the third term the desired correlation after an appropriate change of variable. If the input signals are identical, the correlation term is formed at the point where the signals meet on the detector array. Each pixel of the detector array basically corresponds to a difference in time of arrival of the input signal. A typical electrical signal  $S(T,z)$  produced by the detector array of a TIC and displayed on an oscilloscope is shown in Figure 2.

It has been demonstrated [2] that the peak formed by the correlator appears on a pedestal (see Figure 2) and could be multiplied by a fringe system. The fringe period can vary from infinity to a very small value depending on the configuration of the TIC. Figure 2 a) illustrates a peak with an infinite fringe period and a pedestal produced by the configuration illustrated in Figure 1 if the diffracted signals were propagating in the same direction after mixing. Figure 2 b) illustrates the output produced by the configuration of Figure 1 when a fringe pattern is present because the diffracted signals propagate in different



a)



b)

FIGURE 2: CORRELATION PEAKS ON A PEDESTAL:  
 a) NO MODULATION  
 b) WITH MODULATION

directions after mixing. The individual outputs from each element of the detector array are visible on the oscilloscope trace. The presence of a peak, with or without modulation, indicates that the two input signals A and B are identical and inversely the absence of the correlation peak indicates that the two inputs are different.

The detection is performed by an array of detecting elements having a periodic sensitivity response. The measured and deconvolved sensitivity responses of the Thompson CSF board THX 1061 with the array TH 7805 are illustrated respectively in Figure 3 a) and c). The diffraction pattern that was used to measure the response and to perform the deconvolution is illustrated in Figure 3 b).

It is desirable to enhance the correlation peaks by removing the pedestals shown in Figure 2. The experimental results presented in this technical note were obtained by subtracting two successive frames collected by the detector with a  $180^\circ$  phase shift on one of the signals applied to the Bragg cells for the collection of the second frame. This method is described in details in [2].

### 3.0 DESCRIPTION OF THE SIMULATION

#### 3.1 Format of the Light Distribution

The light distribution produced by the TIC can be described by using the three following elements:

- 1) a triangular envelope of variable width and location,
- 2) a spatial modulation of the triangular envelope and,
- 3) a uniform bias.

The modulation is multiplied with the triangular envelope and that product is added to a uniform bias often referred to as a pedestal.

Let us first consider the origin and the factors affecting the shape of the triangular envelope. The input is assumed to be a binary phase-shift keyed (BPSK) signal. The triangular envelope is formed by the auto correlation of the rectangular chips modulating the input signal. Its width at the base is equal to the length of the bits and is therefore equal to the velocity  $v$  of the acoustic signal in the Bragg cell divided by the bit rate  $B$  used to build the sequence. The apex of the triangular envelope is located at the meeting point of the two input signals and can be found anywhere within the time window of the TIC according to the difference of time of arrival of the signals.

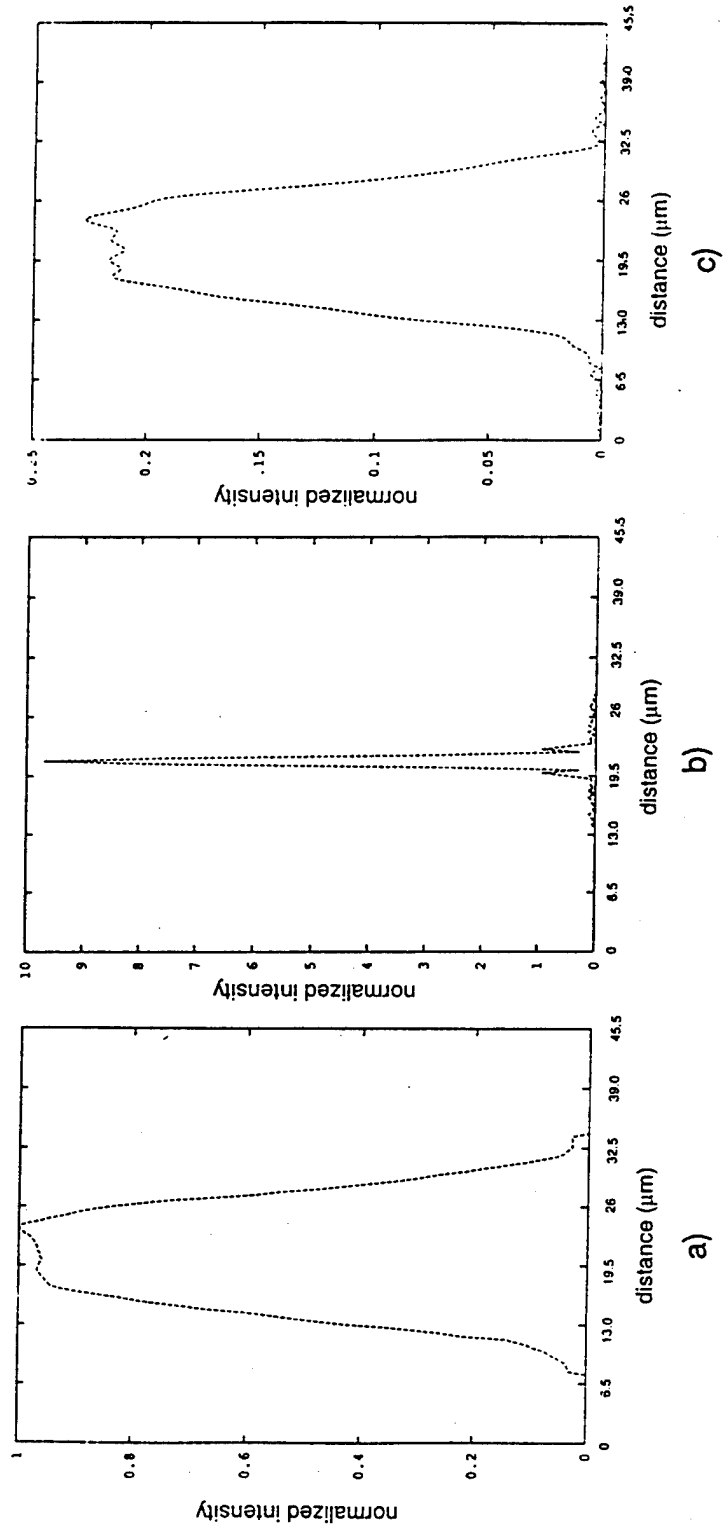


FIGURE 3: a) THE MEASURED SENSITIVITY PROFILE FROM THE THOMPSON CSF DETECTOR ARRAYS  
 b) THE DIFFRACTION PATTERN THAT WAS USED TO SCAN THE ARRAY  
 c) AND THE DECONVOLVED SENSITIVITY PROFILE.

The second element contributing to the TIC output is the spatial modulation of the peak. In the absence of aberration or misalignment of the optical system, the period of the modulation is inversely proportional to the angle between the two beams diffracted by the Bragg cells. The period can vary from infinity, when the two beams are collinear, to a very small value when the angle between the two beams is large. The period and the phase can also be locally affected by the presence of optical aberrations or misalignments of the optical system. The phase of the modulation depends from the phase difference of the signals applied to the Bragg cells.

The third factor contributing to the output of a TIC is the bias that is added to the product of the modulation pattern with the triangular envelope. The biases illustrated in Figure 2 display the characteristic Gaussian shape of the laser beam illuminating the correlator. Consequently, a uniform illumination is desirable to obtain a correlation peak that has the same height on the whole window of operation of the TIC. Techniques to obtain such a distribution have been developed and will be discussed in a further publication.

### 3.2 Detection Process

The light distribution produced by a TIC is detected by an array of elements having a finite size and a specific sensitivity response. The process is modelled by a spatial integration of the energy incident on each element where the incident energy is weighted with the sensitivity response of the detecting elements.

The main factors having an influence on the results of the spatial integration process are the physical size of the detecting elements and its sensitivity profile, that may include a dead-space. The location of the detecting elements of the array relative to the features of the light distribution is also a key factor. The impact of these parameters on the detection of a correlation peak have been studied [7] for the ideal case of no modulation and of perfect adjustment of the relative phase of the input signals.

### 3.3 Description of the Main Programs

A computer simulation was written to study the detection of the light distribution produced by a TIC and two different programs were developed. The simulation is based on an idealized description of the many factors contributing to the detection process. These factors can be classified into three categories.

- 1) the factors describing the light distribution produced by the TIC such as bias, modulation period and phase,

- 2) the parameters of the detector array such as the size and the sensitivity response of the elements and
- 3) the position of the elements of the detector relative to the features of the light distribution being detected.

The first program is called PUBDET. It calculates the energy integrated by each element of the detector array. It is an interactive program that ask the user for values of the following four input parameters whose definition is illustrated in Figure 4:

- 1) the width  $W$ , at the base, of the triangular envelope in number of detecting elements,
- 2) the position  $C$  of the apex of the triangular envelope, in number of samples in one detecting element, measured from the edge of the central element underlying the envelope,
- 3) the period  $P$  of the modulation pattern in number of detecting elements and
- 4) the phase  $\phi$  (in radian) of the modulation pattern at the apex of the triangular envelope

PUBDET first defines the triangular envelope at the location specified by the user. A modulation pattern with the phase and period specified by the user is calculated and multiplied by the triangular envelope and the uniform bias is added. Then the energy reaching each element of the detector array is calculated taking into account the sensitivity response of the elements. Finally, the program generates the data and the files required to produce graphic outputs of which Figure 5 is a typical example. From top to bottom, first row a) illustrates the modulation pattern whose amplitude oscillates between  $-1$  and  $+1$ . The row b) illustrates the triangular envelope whose minimum and maximum amplitude are respectively  $-1$  and  $+1$  and the row c) displays the product rows a and b, added to a uniform bias of amplitude one. The row d) illustrates the position of the central detecting element of the array and its sensitivity response. The last row, row e) presents the histogram of the energy collected by each element.

The second program is called DISEL. It calculates the intensity on the element collecting the most energy for all the positions, of the apex of the triangular envelope on the central detecting element. It is an interactive program that requires from the user the values of the following variables:

- 1) the width  $W$ , at the base, of the triangular envelope in number of detecting elements,
- 2) the period  $P$  of the modulation pattern in number of detecting elements.



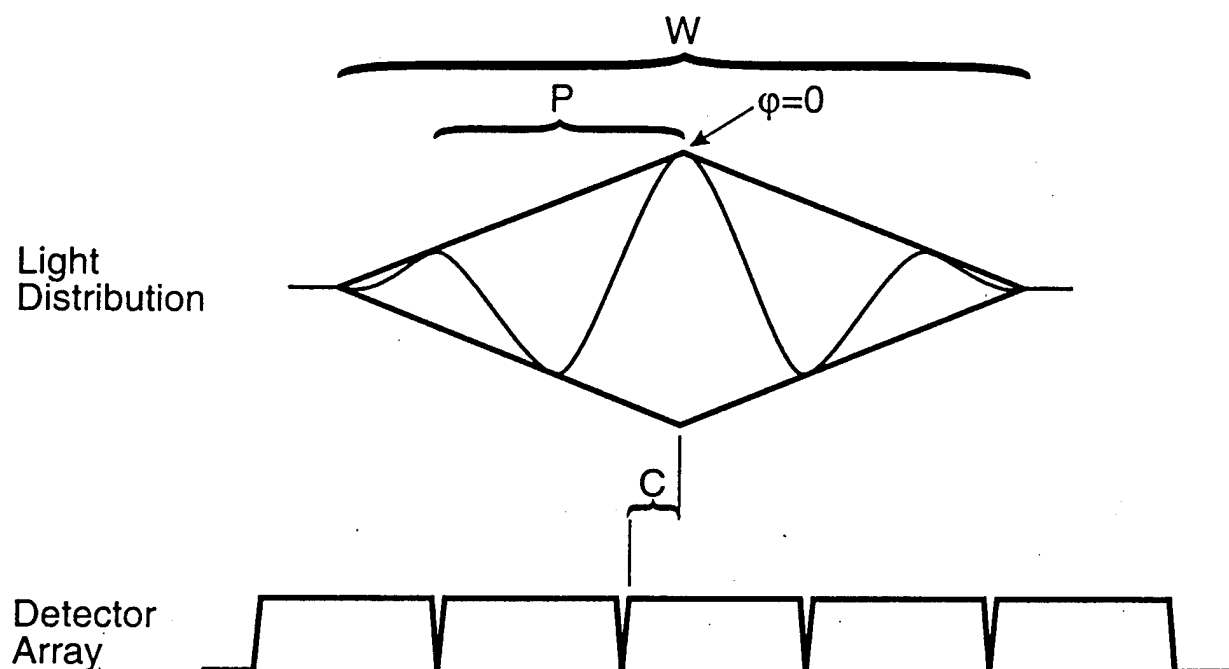


FIGURE 4: DEFINITION OF THE INPUT PARAMETERS FOR THE COMPUTER SIMULATION

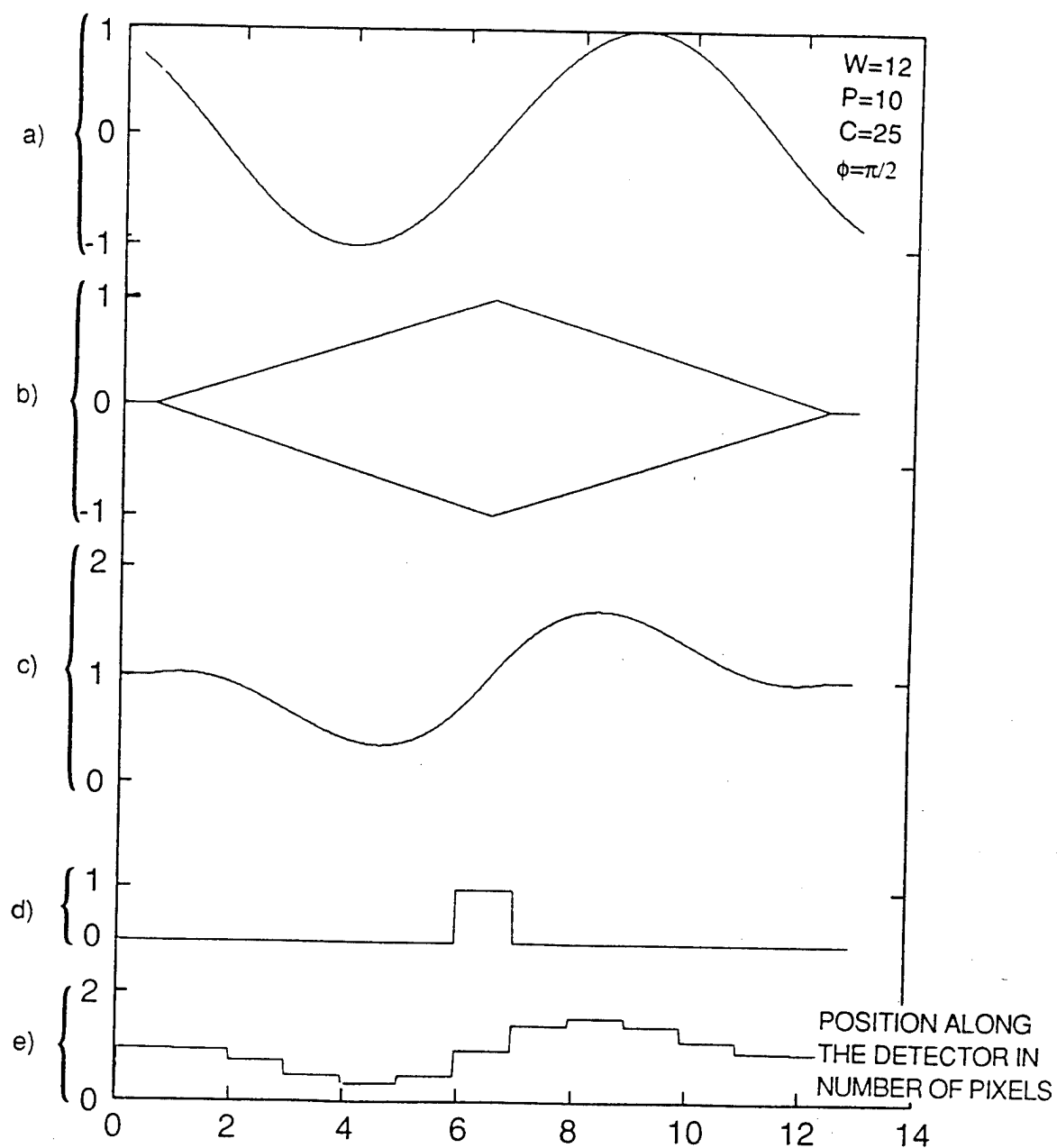


FIGURE 5: EXAMPLE OF THE OUTPUT FROM PUBDET WITH  $W=12$ ,  $P=10$ ,  $C=25$  AND  $\phi=\pi/2$  FOR A RECTANGULAR SENSITIVITY RESPONSE OF THE DETECTOR.

The intensity on the element collecting the most energy is calculated for  $\phi=0$  and  $\phi=\pi/2$  which are respectively, the conditions producing the tallest and the smallest peak when a modulation is present. There are fifty equidistant sampling points on each element.

This program also calculates, for comparison purposes, the ideal case of no modulation when the phase difference between the input signals is set to obtain the strongest signal. This last case produces the tallest peaks and is the only one discussed in the literature on TIC [2-6]. The triangular envelope previously specified by the operator is used in that last case. Figure 6 is a typical output from DISEL. The higher curve corresponds to the ideal case with no modulation while the second and third curves from the top corresponds to a modulation with  $\phi=0$  and  $\phi=\pi/2$  respectively.

#### 4.0 FEATURES OF THE DETECTION PROCESS

Let us consider a few examples to illustrate the salient features of the detection process of a TIC. Two main factors are considered in this section, namely, the effect of the phase difference between the input signals and the location of the detecting elements with respect to the features of the light distribution. The crucial importance of the period of the modulation will become evident from the discussion.

First, let us consider the particular case arising when a modulation is present. Figure 7(a) illustrates the output of a TIC, for two signals with a relative phase difference of  $0^\circ$  arriving simultaneously and producing a peak in the middle of the time-window. Figure 7(b) illustrates the same situation, but for a  $90^\circ$  phase difference of the RF input signals. The effect of the different phase between the signals is to shift the modulation. As the triangular envelope stays at the same location, its product with the modulation pattern, can be quite different.

If the relative phase of the RF inputs is constant, a similar effect could be produced by a displacement of the triangular envelope caused by a different time of arrival of the RF input signals. The triangular envelope slides over the fixed modulation pattern according to the difference of time of arrival of the RF input signals. Its product with the modulation pattern varies accordingly and the energy collected by the elements of the detector depends on the location of the elements of the detector relatively to the modulated triangular envelope.

SIGNAL ON THE PIXEL  
COLLECTING THE MOST  
ENERGY

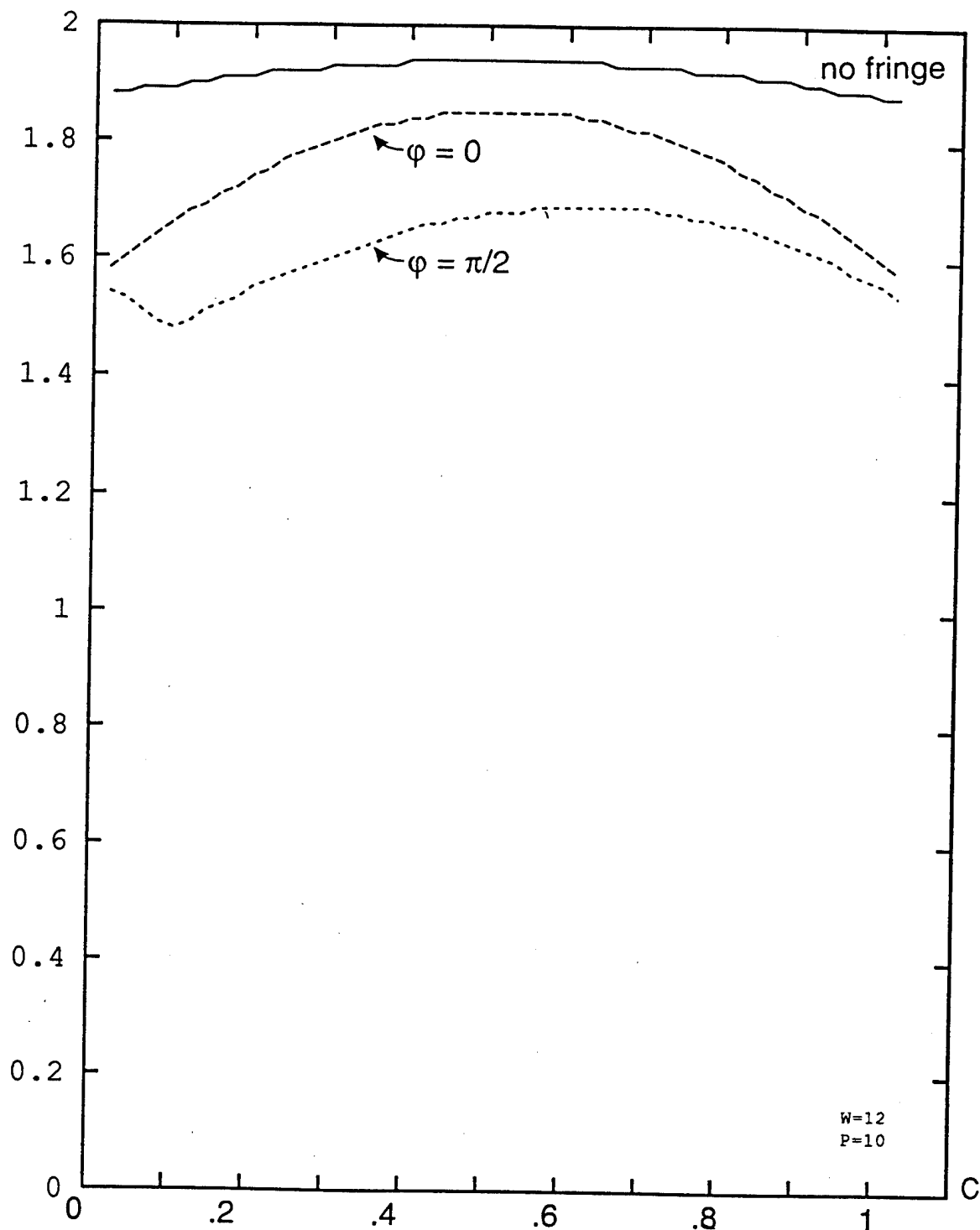


FIGURE 6: EXAMPLE OF THE OUTPUT FROM DIESEL WITH W=12 AND P=10 FOR A RECTANGULAR SENSITIVITY RESPONSE OF THE DETECTOR

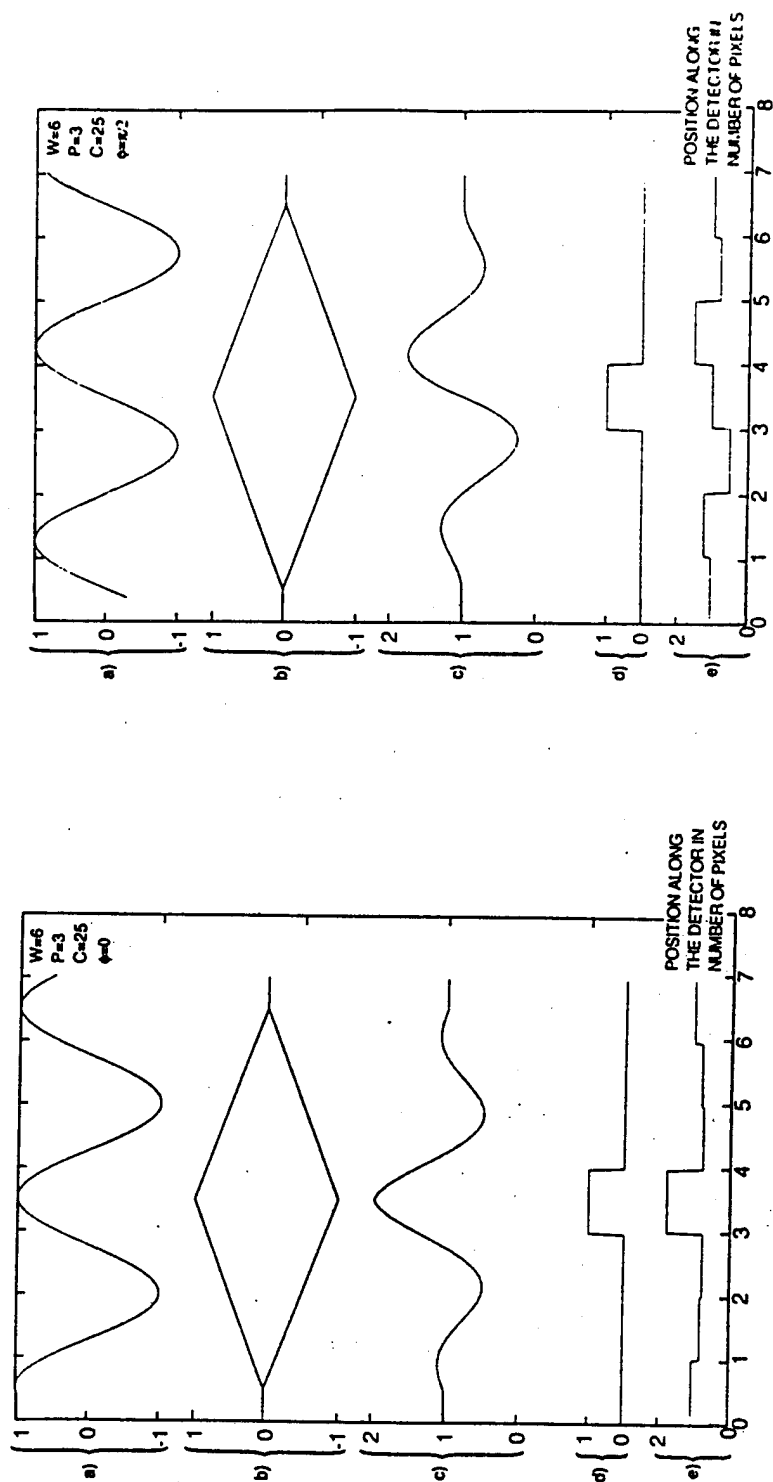


FIGURE 7: OUTPUT FROM A TIME-INTEGRATING CORRELATOR WITH MODULATION FOR  $W=6$ ,  $C=25$  AND  $\phi=0$  AND  $\pi/2$  FOR A RECTANGULAR SENSITIVITY RESPONSE OF THE DETECTOR.

When there is no modulation, a uniform background whose amplitude depends on the relative phase of the input signals (Figure 8) is produced. Such a uniform background can be described as a modulation with an infinite period. For a phase difference of  $0^\circ$  or  $180^\circ$ , the contributions to the peaks are, respectively, a maximum and a minimum (Figure 8a and 8c). The contribution to the peak is null if the phase difference is  $90^\circ$  (Figure 8b). The formation of detectable peak thus requires a tight control of the phase difference between the input RF signals.

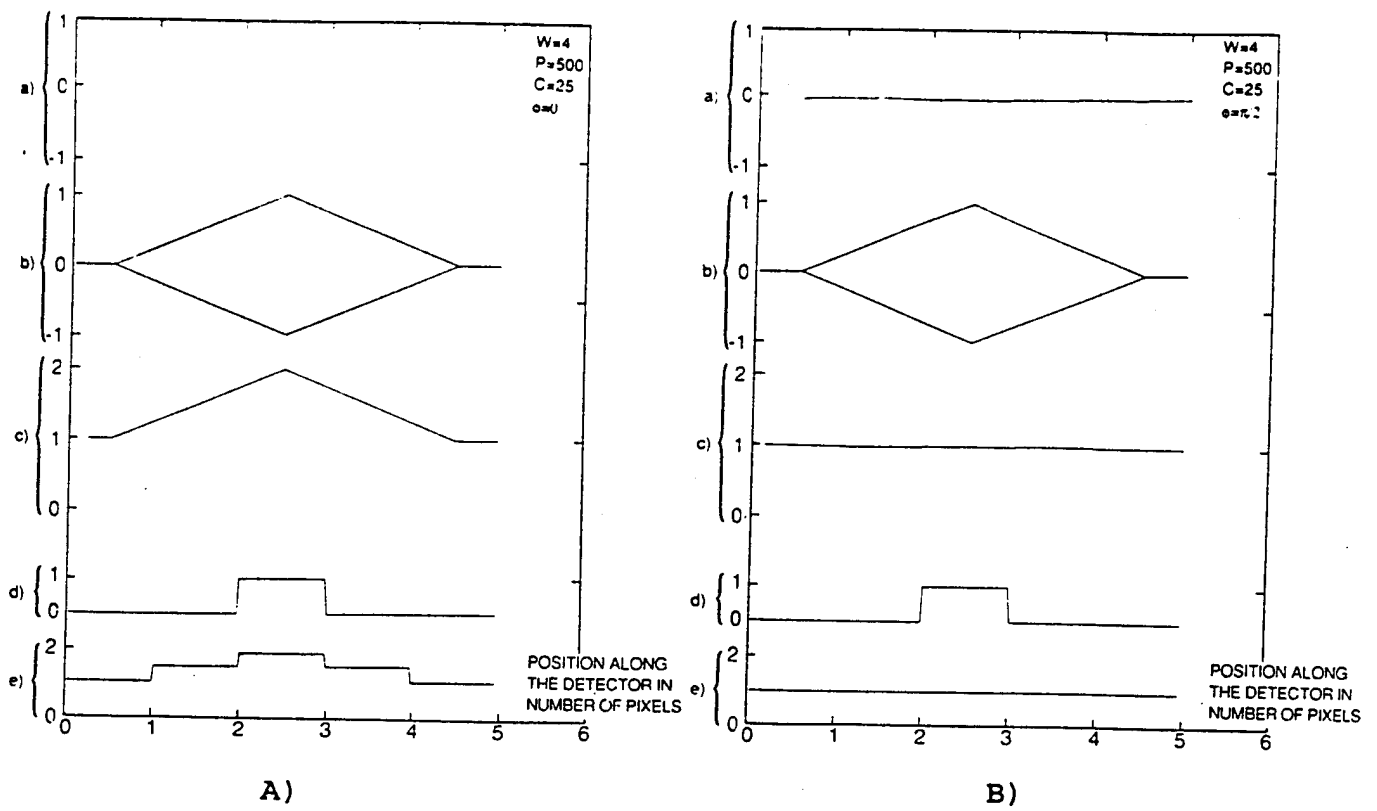
#### 4.1 Effects of the Location of the Detecting Elements

Let us now consider the effect of the location of the detecting elements on the detection of a modulated triangular envelope. Figure 9 illustrates the detection process for a width  $W=4$  of the triangular envelope. Fifty equispaced samples are calculated on each detecting element and the array is displaced from a position 0 to 50 samples by increments of 10. The results for a case where no modulation is present are summarized in Figure 10. The energy accumulated on the element receiving the most energy has been plotted as a function of the position of the array.

Another case with no modulation and a triangular envelope with a width  $W=10$  is illustrated in Figure 11. The array is displaced from a position 0 to 50 by increments of 10. The situation is summarized in Figure 12 where the energy accumulated on the element receiving the most energy has been plotted as a function of the displacement of the array. The comparison of Figure 10 and 12 indicates that a larger width of the triangular envelope leads to higher peaks whose amplitude is less affected by the different positions of the detecting elements. However, wider triangular envelopes are also associated with smaller chip rates and reduced capabilities to process data.

#### 4.2 Effects of the Phase Difference Between the RF Input Signals

Ideally, the output of a TIC should be free of optical phase error and the phase difference of the input signals should be adjusted to produce a maximum amplitude. However, these conditions are quite difficult to achieve and maintain. It requires the utilization of diffraction limited optical components, the capability to achieve and maintain near perfect alignment of the whole optical system and the precise adjustment of the phase difference of the signals applied to the Bragg cells. It has also been demonstrated that the changes of acoustic velocity in the Bragg cells associated with small temperature changes can cause the formation of a modulation pattern [8]. Tight temperature control is required [8] to prevent this problem.



C)

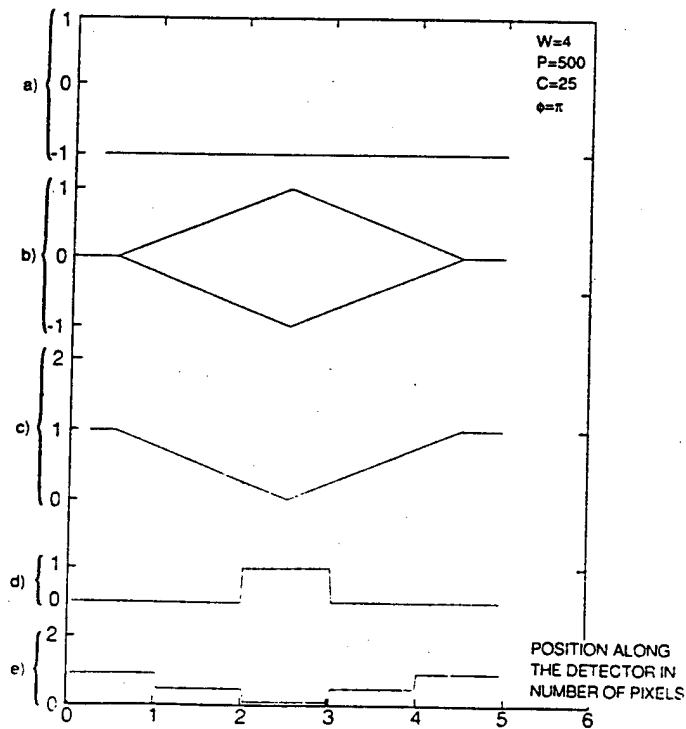


FIGURE 8: OUTPUT FROM A TIME-INTEGRATING CORRELATOR FOR  $W=4$ ,  $C=25$ ,  $P=500$  AND  $\phi=0$  AND  $\pi/2$  FOR A RECTANGULAR SENSITIVITY RESPONSE OF THE DETECTOR.

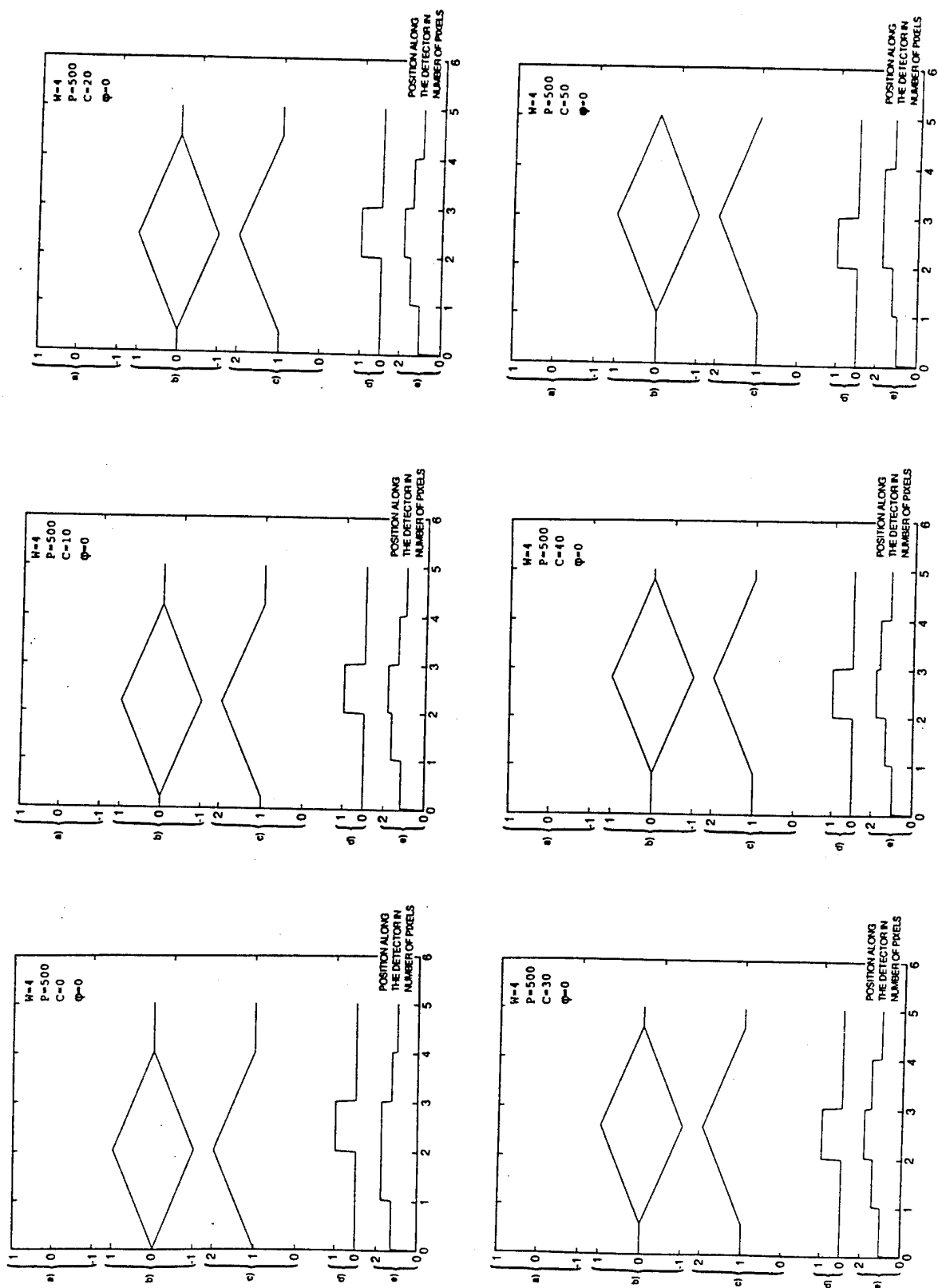


FIGURE 9: OUTPUT FROM A TIME-INTEGRATING CORRELATOR FOR  $W=4$ ,  $F=500$ ,  $\phi=0$  AND  $C=0, 10, 20, 30, 40$  AND  $50$  FOR A RECTANGULAR SENSITIVITY RESPONSE OF THE DETECTOR



SIGNAL ON THE PIXEL  
COLLECTING THE MOST  
ENERGY

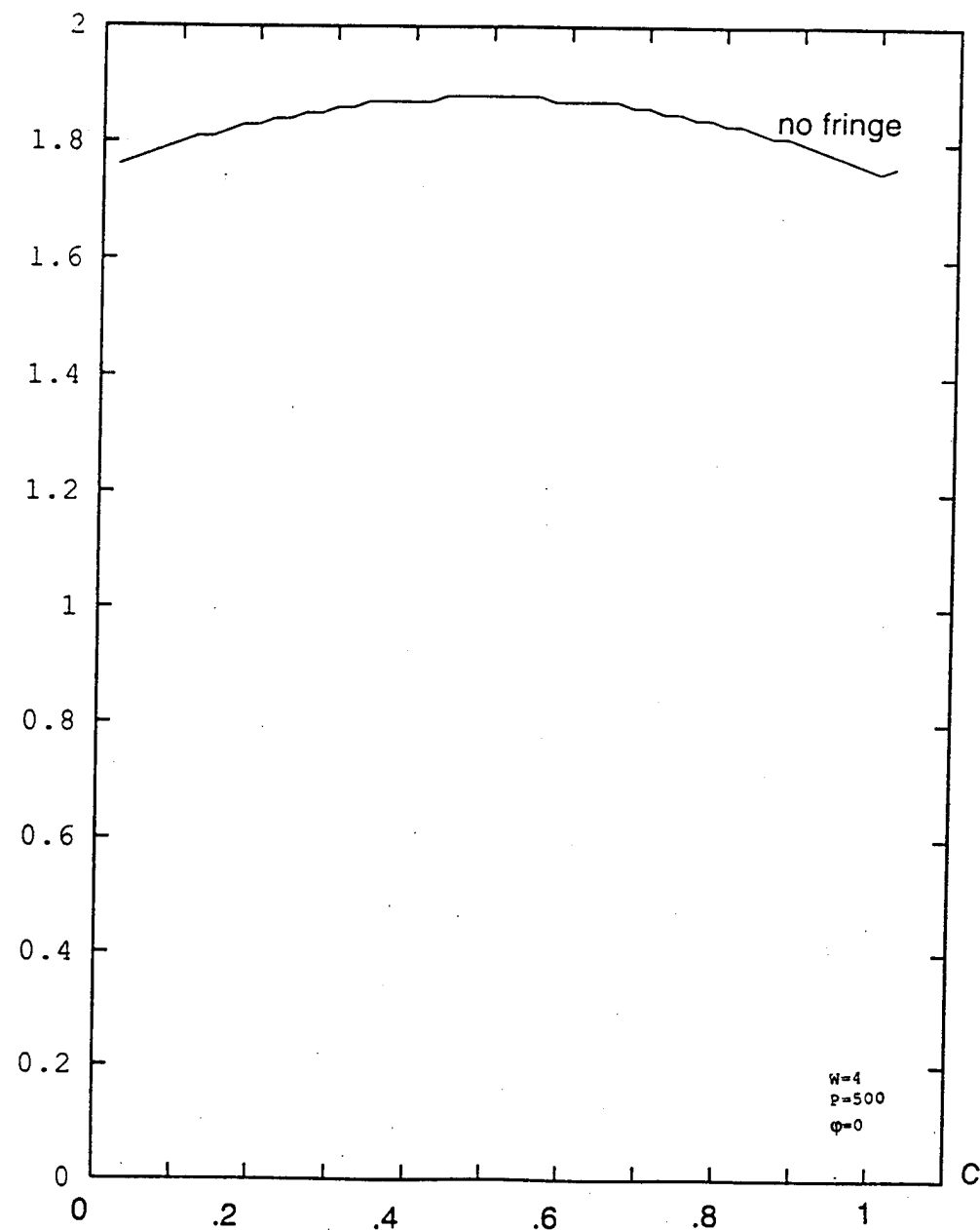


FIGURE 10: AMPLITUDE OF THE PEAK AS A FUNCTION OF THE POSITION OF THE APEX OF THE TRIANGULAR ENVELOPE ON THE DETECTING ELEMENT WITH A VERY LARGE FRINGE PERIOD FOR  $W=4$ ,  $P=500$ ,  $\phi=0$  FOR A RECTANGULAR SENSITIVITY RESPONSE OF THE DETECTOR

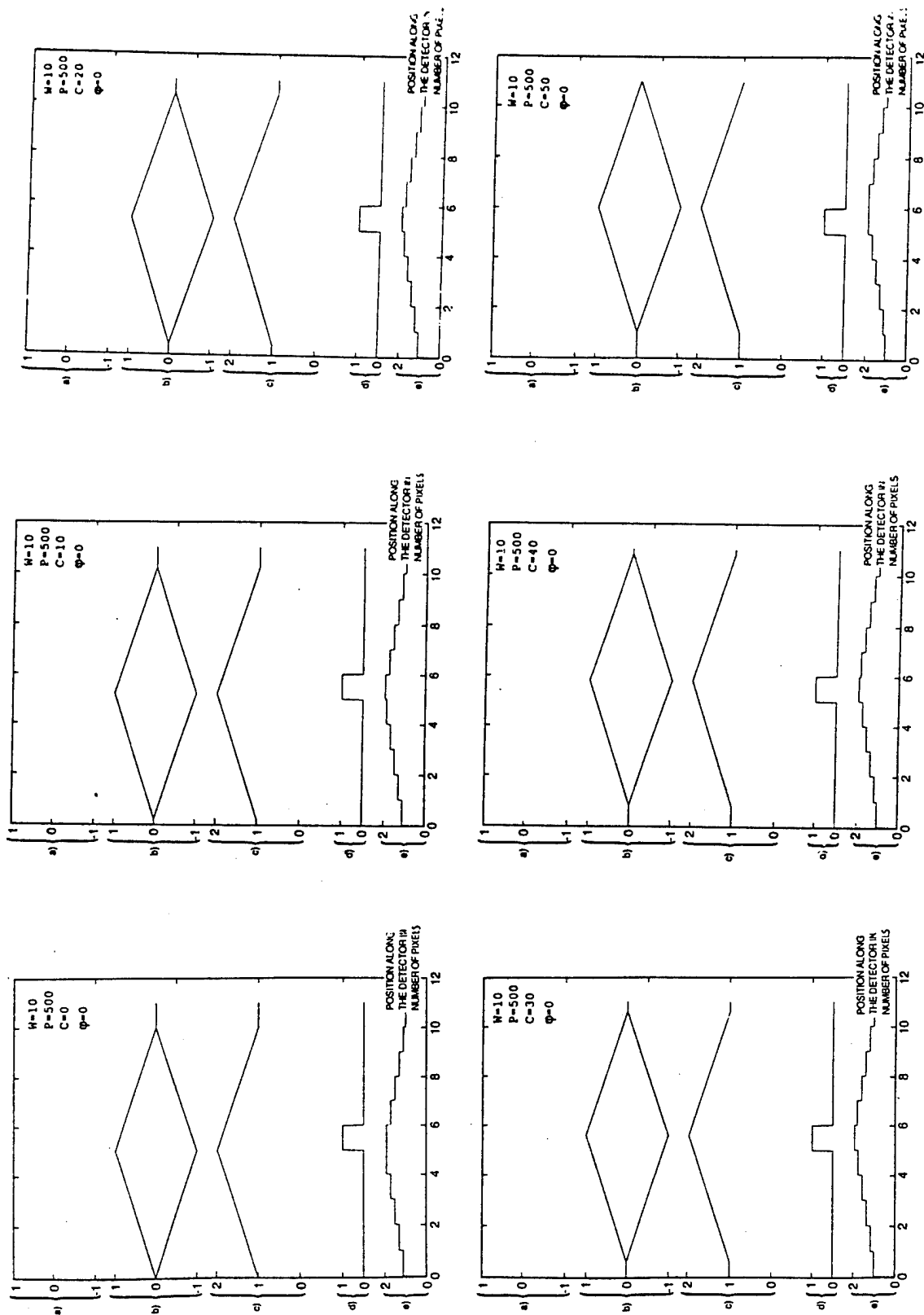


FIGURE 11: OUTPUT FROM A TIME-INTEGRATING CORRELATOR FOR  $W=10$ ,  $P=500$ ,  $\phi=0$  AND  $C=0, 10, 20, 30, 40$  AND  $50$  FOR A RECTANGULAR SENSITIVITY RESPONSE OF THE DETECTOR

POSITION ALONG  
THE DETECTOR IN  
NUMBER OF PIXELS

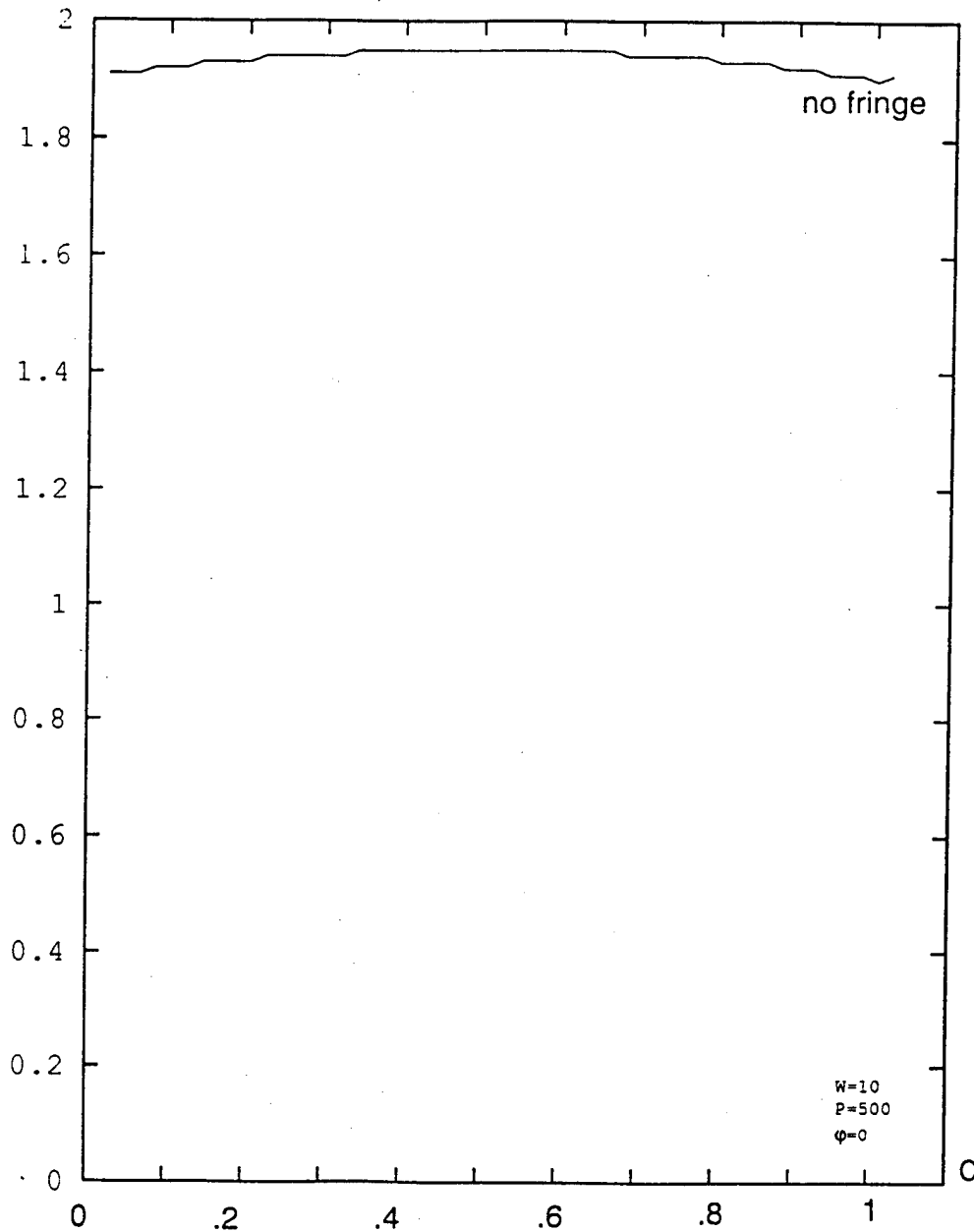


FIGURE 12: AMPLITUDE OF THE PEAK AS A FUNCTION OF THE POSITION OF THE APEX OF THE TRIANGULAR ENVELOPE ON THE DETECTING ELEMENT: WITH A VERY LARGE FRINGE PERIOD FOR  $W=10$ ,  $P=500$ ,  $\phi=0$  FOR A RECTANGULAR SENSITIVITY RESPONSE OF THE DETECTOR

Let us assume that a large period modulation is produced by any or a combination of the factors mentioned in the previous paragraph. The situation is illustrated in Figure 13 where two extreme results of the detection process are illustrated for a large modulation period. Figure 13a corresponds to a combination of parameters with  $\phi=0$  that leads to the formation of a detectable peak. Figure 13b differs only by the location of the apex of the triangular envelope relative to the modulation or equivalently by the phase of the modulation pattern ( $\phi=\pi/2$ ). In this last use, it is difficult to detect the peak. The amplitude of the peak as a function of the position of the apex of the triangular envelope relative to the detecting element is illustrated in Figure 13c for  $\phi=0$  and  $\phi=\pi/2$ . The energy in the peak is about 1.35 for  $\phi=\pi/2$  and the amplitude of the peak produced is, at best, difficult to detect and a blind spot in the field of view of the correlator is generated. It is obviously an unacceptable feature for a system that is expected to produce reliable peak detection. Operating a TIC with no modulation of the triangular envelope can only produce reliable peak detection if there is an absolutely perfect control of the optical and RF phase of the signals.

## 5.0 OPTIMAL DETECTION PARAMETERS

Further studies of the detection process with the simulation have established that it is possible to reach a compromise where stable performance of a fair quality is traded against unpredictable performances that are either excellent or very poor. To eliminate the occurrence of disasters in the detection process we purposefully produce at the output of the TIC a modulation whose period is calculated to produce peaks with an acceptable amplitude variation for all positions of the detecting elements relative to the modulation and the triangular envelope. The peak height is then always above a minimum set by the user.

### 5.1 For a Uniform Sensitivity Response

The amplitude of the peak has been calculated for a uniform sensitivity response of the detecting element. A large range of values for the width  $W$  of the triangular envelope and for the period  $p$  of the modulation was systematically explored. This approach allowed to locate combination of parameters producing correlation peaks whose amplitude was sufficiently high and sufficiently constant for all positions of the peak across the detecting element.

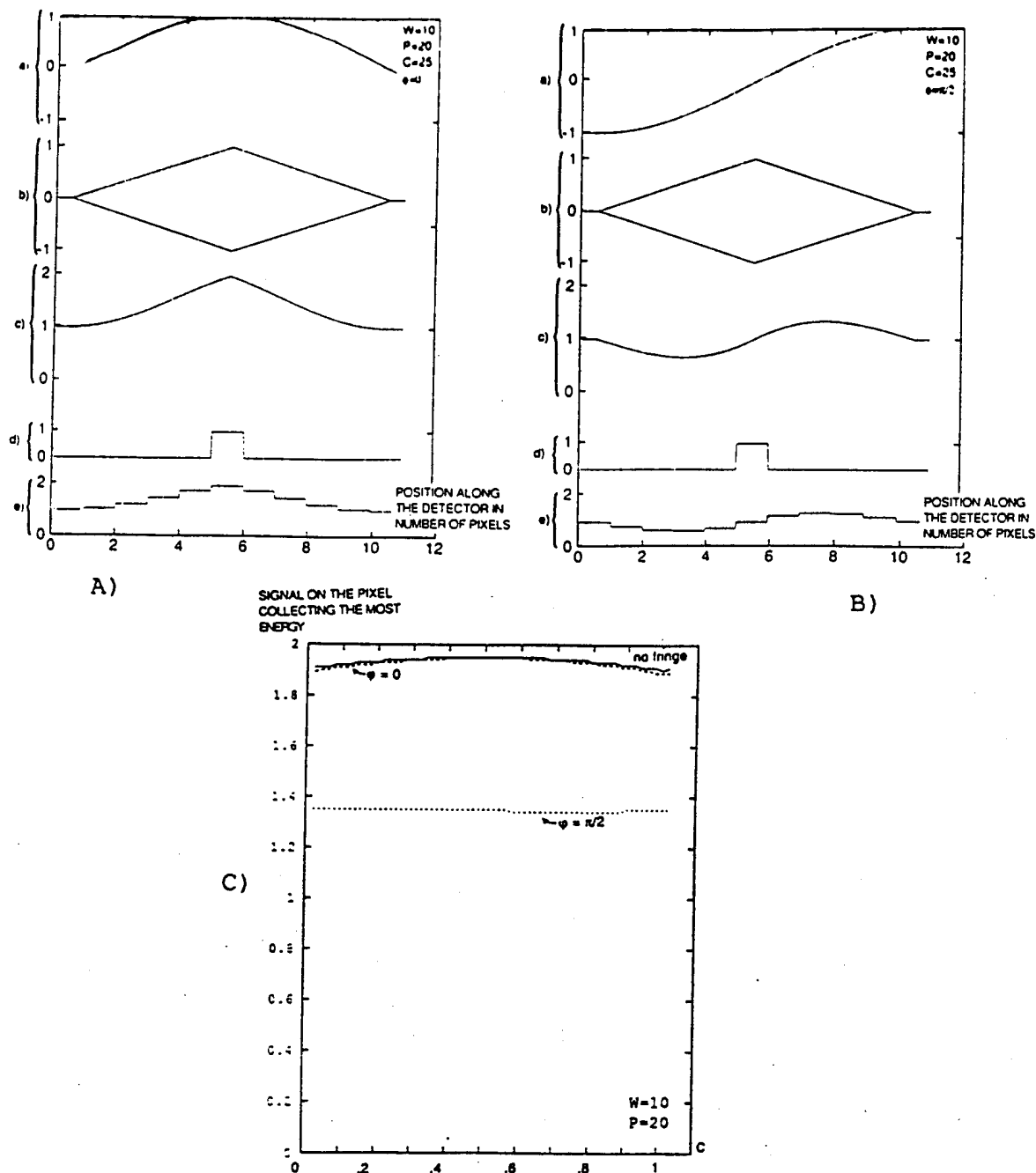


FIGURE 13:

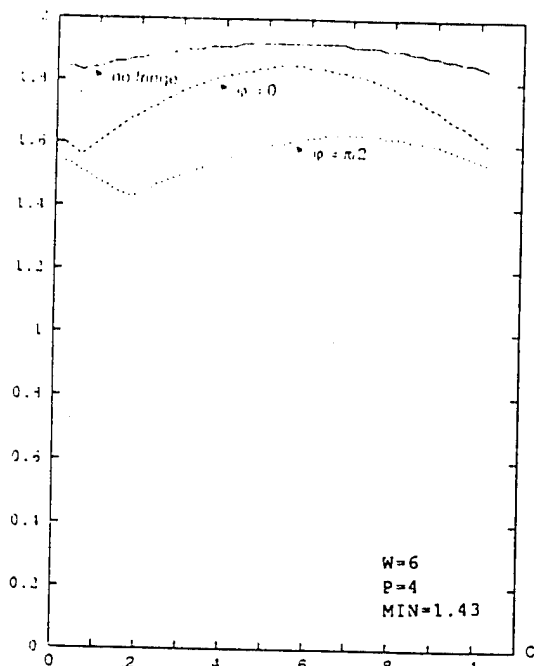
OUTPUT FROM A TIME-INTEGRATING CORRELATOR FOR A RECTANGULAR SENSITIVITY RESPONSE OF THE DETECTOR AND WITH

A)  $W=10$ ,  $C=25$ ,  $P=20$  AND  $\phi=0$ .

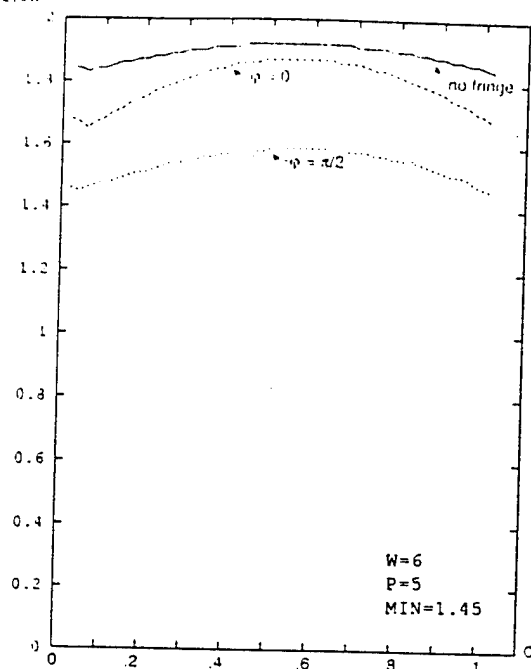
B)  $W=10$ ,  $C=25$ ,  $P=20$  AND  $\phi=\pi/2$ .

C) AMPLITUDE OF THE PEAK AS A FUNCTION OF THE POSITION OF THE APEX OF THE TRIANGULAR ENVELOPE ON THE DETECTING ELEMENT: THE MODULATION PERIOD IS VERY LARGE AND  $W=10$ ,  $P=5000$ ,  $C=0$  AND  $\phi=\pi/2$ .

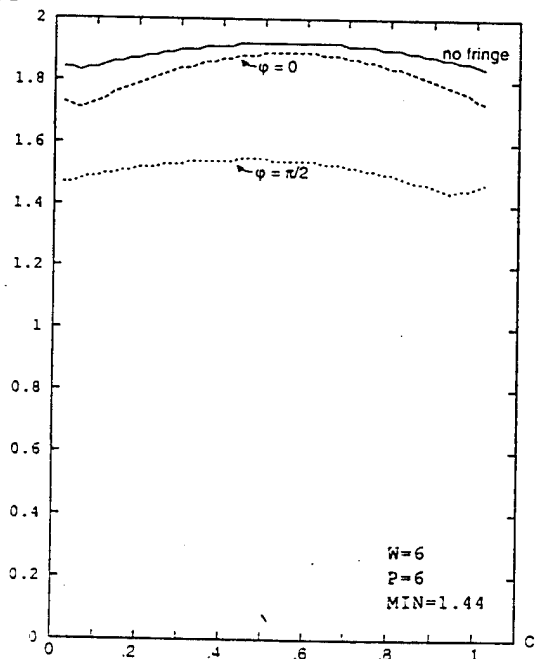
SIGNAL ON THE PIXEL  
COLLECTING THE MOST  
ENERGY



SIGNAL ON THE PIXEL  
COLLECTING THE MOST  
ENERGY



SIGNAL ON THE PIXEL  
COLLECTING THE MOST  
ENERGY



SIGNAL ON THE PIXEL  
COLLECTING THE MOST  
ENERGY

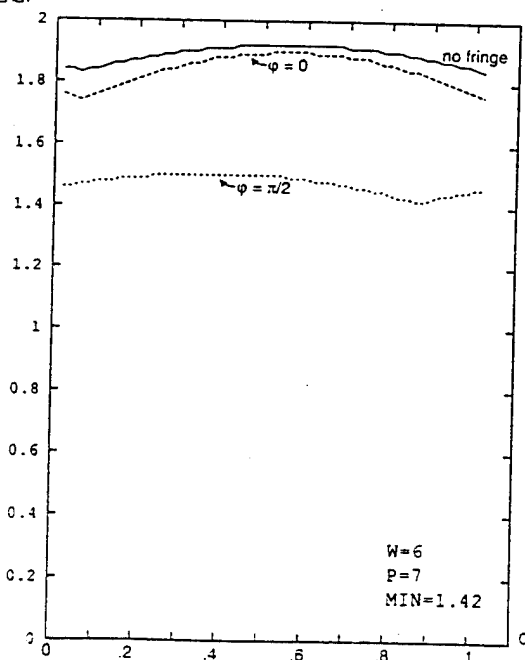
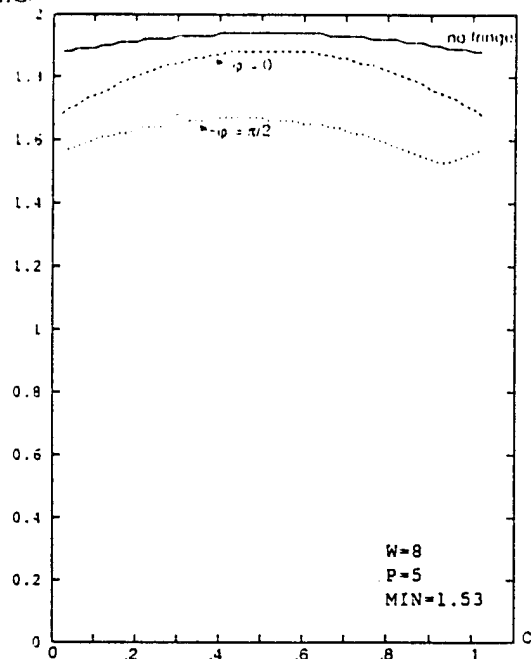
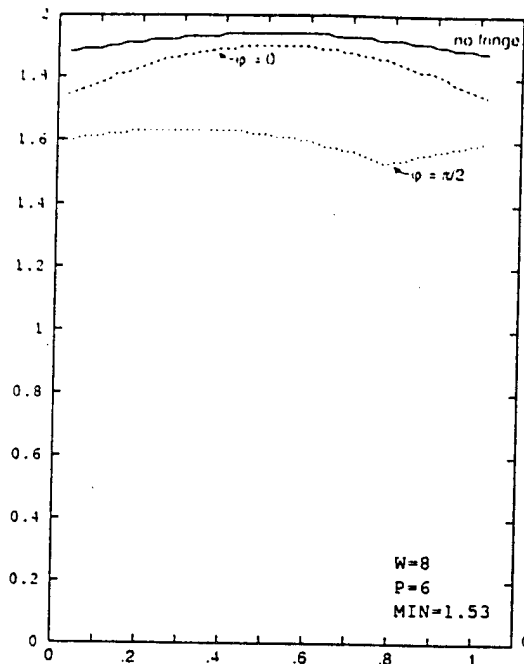


FIGURE 14: AMPLITUDE OF THE PEAK AS A FUNCTION OF THE POSITION OF THE APEX OF THE TRIANGULAR ENVELOPE ON THE DETECTING ELEMENT FOR  $W=6$  AND  $P=4, 5, 6$  AND  $7$  FOR A RECTANGULAR SENSITIVITY RESPONSE

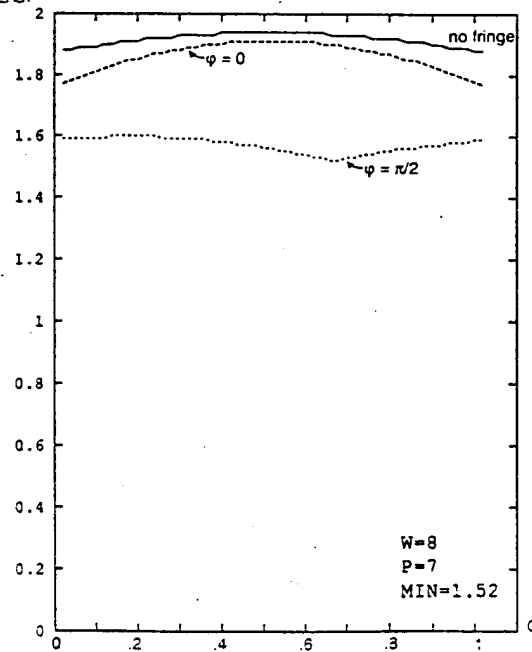
SIGNAL ON THE PIXEL  
COLLECTING THE MOST  
ENERGY



SIGNAL ON THE PIXEL  
COLLECTING THE MOST  
ENERGY



SIGNAL ON THE PIXEL  
COLLECTING THE MOST  
ENERGY



SIGNAL ON THE PIXEL  
COLLECTING THE MOST  
ENERGY

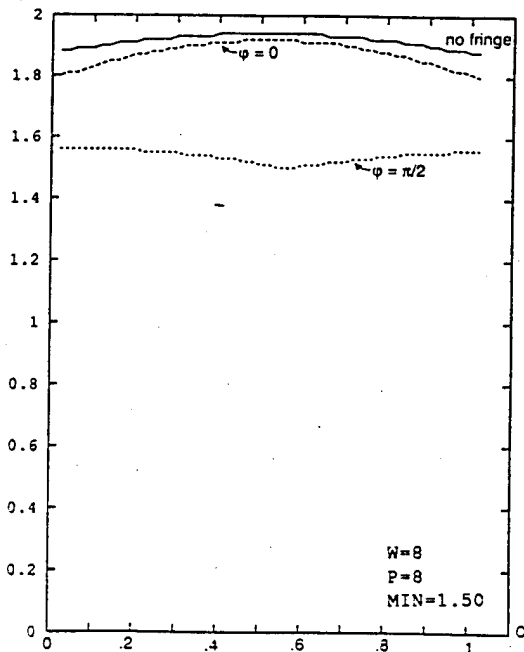
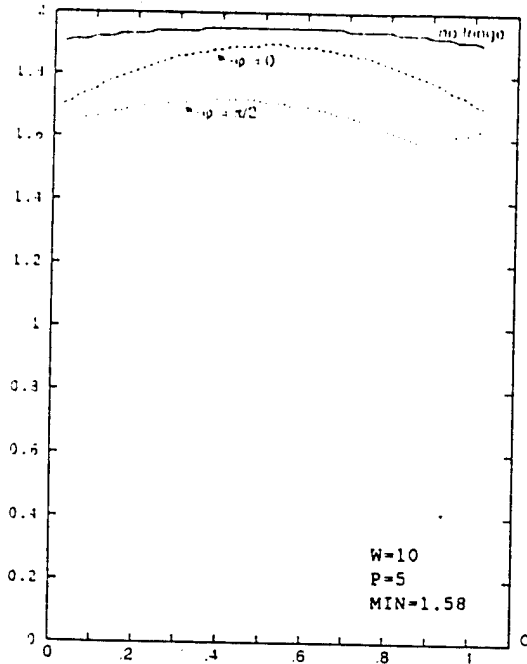
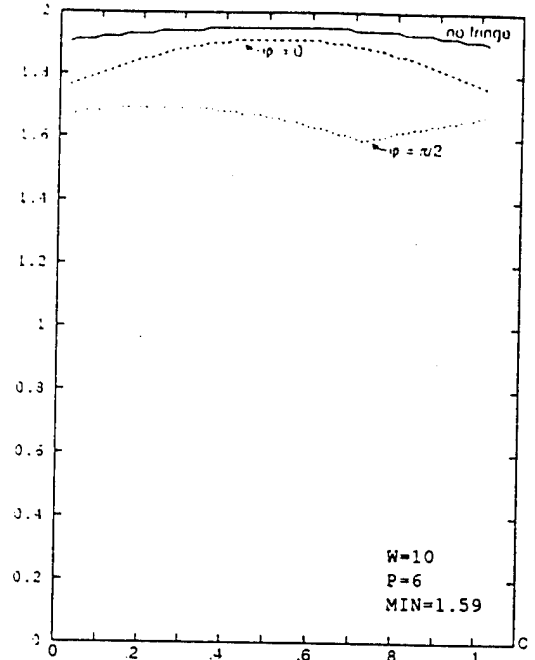


FIGURE 15: AMPLITUDE OF THE PEAK AS A FUNCTION OF THE POSITION OF THE APEX OF THE TRIANGULAR ENVELOPE ON THE DETECTING ELEMENT FOR  $W=8$  AND  $P=5, 6, 7$  AND  $8$  FOR A RECTANGULAR SENSITIVITY RESPONSE

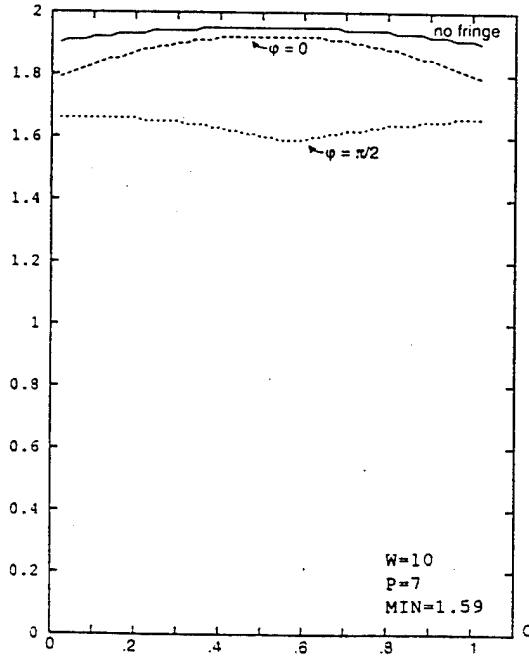
SIGNAL ON THE PIXEL  
COLLECTING THE MOST  
ENERGY



SIGNAL ON THE PIXEL  
COLLECTING THE MOST  
ENERGY



SIGNAL ON THE PIXEL  
COLLECTING THE MOST  
ENERGY



SIGNAL ON THE PIXEL  
COLLECTING THE MOST  
ENERGY

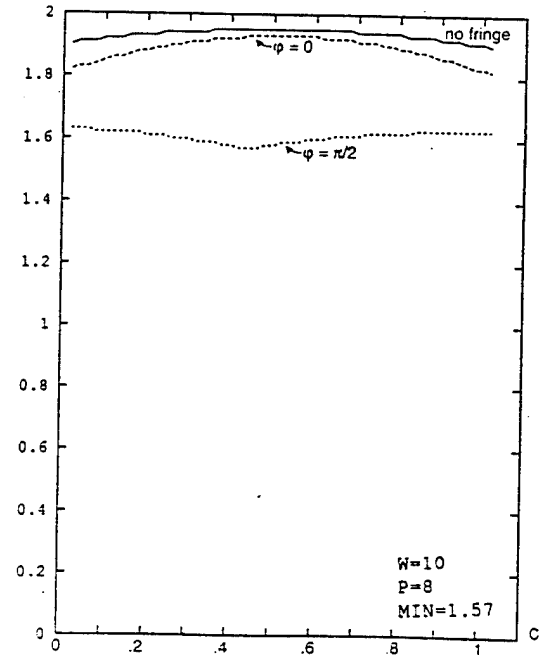
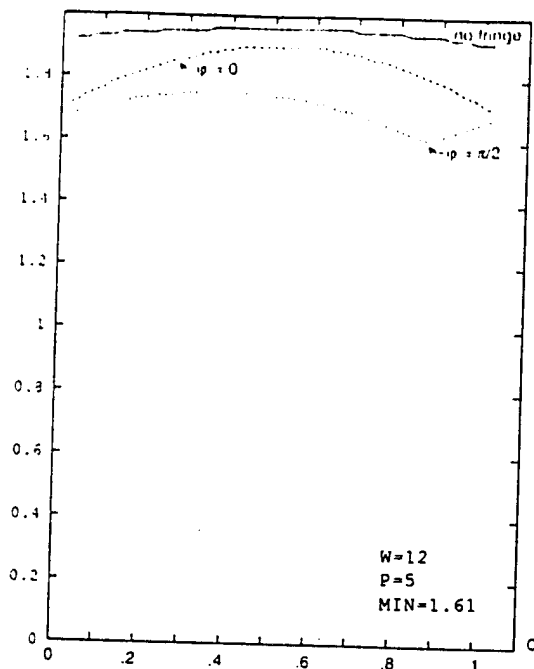


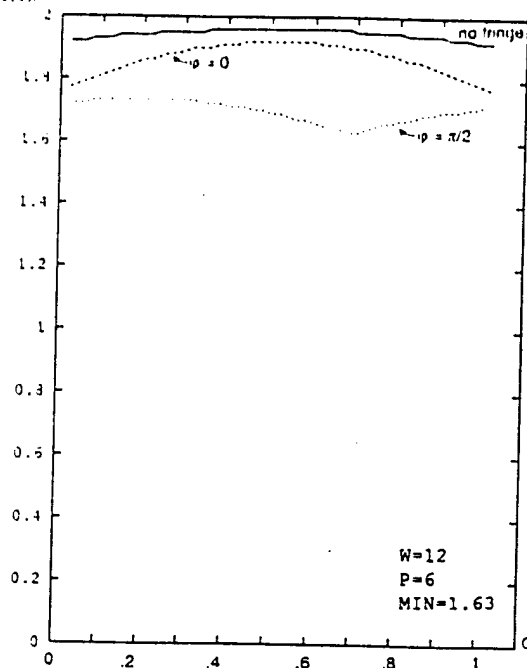
FIGURE 16: AMPLITUDE OF THE PEAK AS A FUNCTION OF THE POSITION OF THE APEX OF THE TRIANGULAR ENVELOPE ON THE DETECTING ELEMENT FOR  $W=10$  AND  $P=5, 6, 7$  AND  $8$  FOR A RECTANGULAR SENSITIVITY RESPONSE



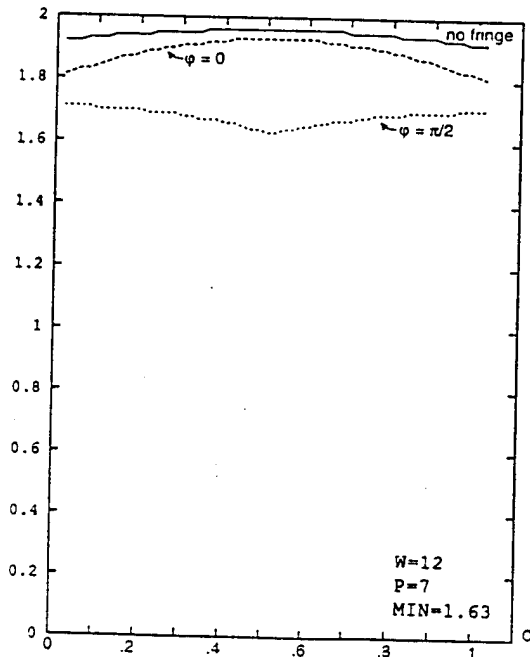
SIGNAL ON THE PIXEL  
COLLECTING THE MOST  
ENERGY



SIGNAL ON THE PIXEL  
COLLECTING THE MOST  
ENERGY



SIGNAL ON THE PIXEL  
COLLECTING THE MOST  
ENERGY



SIGNAL ON THE PIXEL  
COLLECTING THE MOST  
ENERGY

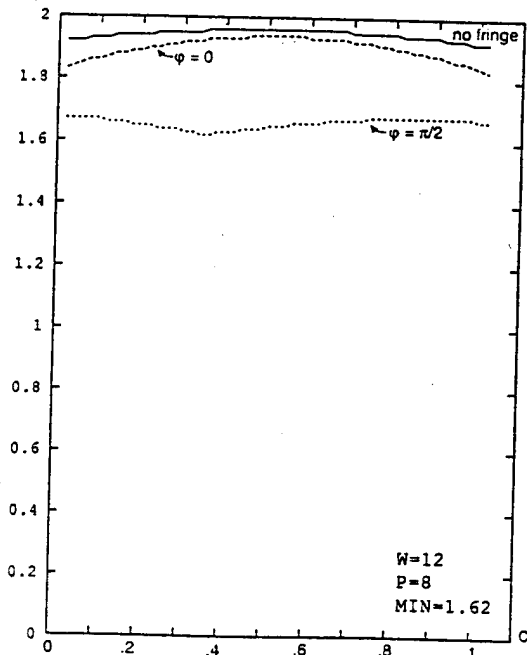


FIGURE 17: AMPLITUDE OF THE PEAK AS A FUNCTION OF THE POSITION OF THE APEX OF THE TRIANGULAR ENVELOPE ON THE DETECTING ELEMENT FOR  $W=12$  AND  $P=5, 6, 7$  AND  $8$  FOR A RECTANGULAR SENSITIVITY RESPONSE

Figures 14, 15, 16 and 17 present the amplitude of the peak as a function of the position of the apex of the triangular envelope on the detecting element for the combinations of parameters W and P giving the best results. In all cases the calculations have been made for the values  $\phi=0$  and  $\phi=\pi/2$  of the modulation at the apex of the triangular envelope. The ideal case of a uniform background with no modulation and a perfect adjustment of the relative phase of the two input signals is added for comparison purposes.

The results illustrated in Figures 14 to 17 allow to observe a trend towards higher peak amplitude with increasing values of the width W of the triangular envelope. A trend towards better peak amplitude uniformity with increasing modulation period P can also be observed. However, one has to remember that W is inversely proportional to the chip rate of the data being processed, so large values of W leads to small values of chip rate and thus to a severe limitation of the processing speed of the correlator. A compromise has to be reached between the processing speed of the correlator and the value of the amplitude and the amplitude uniformity of the peak. The particular choice of W will depends on the speed and peak detection requirements of the system considered. Once an appropriate value for W is selected, the best value of the modulation period P should be chosen accordingly. The selection of the parameters should be based on the results obtained from the simulation and cannot be reduced to an analytical formula.

One particularly important feature of the detection process illustrated in Figures 14 to 17 is the graceful degradation of the amplitude of the peak when the parameters W and P drift from their optimal values. The parameter that is the most likely to drift from its set value is the modulation period P. This is so because the presence of phase error produced by aberration, temperature change [8] or misalignment of the optical components of the system cause alteration of the modulation period of the output. The graceful deterioration is illustrated by the following example. For W=10 (see figure 16), the amplitude of the correlation peak is 1.59 for a modulation period of six or seven pixels. However, if the value of p was to become 5 or 8, the minimum peak amplitude would be 1.58 and 1.57 respectively. It was also demonstrated [8] that the amplitude of the peak produced by the detection of a modulation is very resistant to temperature change. This is in strong contrast with the case where there is no modulation where the amplitude of the peak is very sensitive to temperature change [8].

## 5.2 For the Thompson CSF Detector

The simulation was used to calculate the amplitude of the peak when the detection is performed with a Thompson CSF board THX 1061 and the array TH 7805. The measured [9] and deconvolved

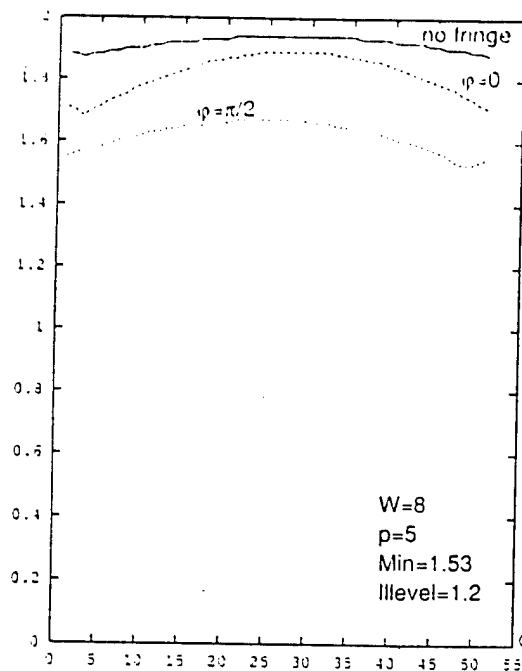
sensitivity responses of the Thompson CSF detector were illustrated respectively in Figure 3 a) and c). The diffraction pattern used to measure the response and to perform the deconvolution is illustrated in Figure 3 b) and the calculation involved are described in Appendix A. Optimal conditions of operation were found by using the methodology for the rectangular response. The amplitude of the peak, as a function of the position of the apex of the triangular envelope for  $W=8$  and  $p=5,6,7$  and  $8$ , is illustrated in Figure 18. One notices that the curves are lower than those of Figure 15 for the rectangular response with the same parameters. This is due to the fact that the Thompson CSF sensitivity response collects less light than the corresponding rectangular profile. This effect can be compensated for by increasing the illumination level by a factor of 1.2. Figure 19 illustrates the curves obtained after the adjustment: they are almost identical to the case of the rectangular sensitivity response used with the same detection parameters (see Figure 15). One can thus conclude that the specific shape of the detecting element response is not a critical parameter of the detection process if proper adjustments of the illumination levels are made.

## 6.0 EXPERIMENTAL VERIFICATION

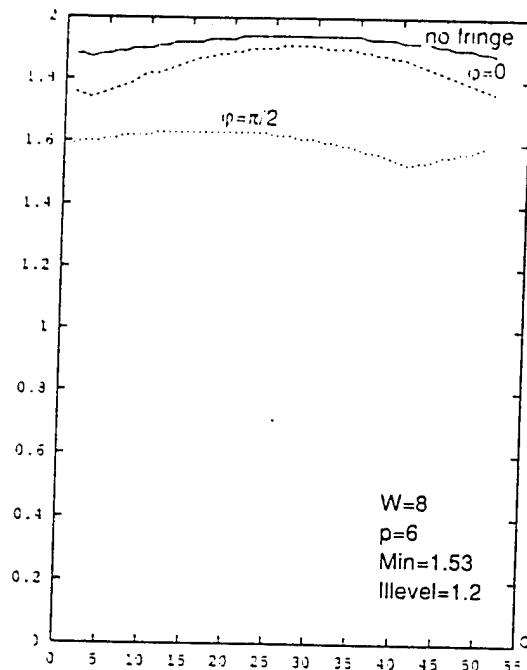
Experimental verifications of the performances of the detection process described in the previous sections were performed with the tandem correlator illustrated in Figure 1. The parameters of the system were selected to produce peaks with amplitude varying between 1.45 and 1.9 by setting the width of the triangular envelope to  $W=6$  and the period of the modulation to  $P=5$  (Figure 14). The controls of the TIC are such that it is possible to change the phase of the RF input to one of the Bragg cells. The relative phase of the two input signals is then altered, although the absolute phase difference between the signals is not known. It is also possible to control the angle between the beams produced by the holographic beam splitter and it was set to produce a modulation period of five pixels. However, in real systems, parameters such as the location of the modulation pattern relative to the apex of the triangular envelope and the position of the detecting elements relative to the triangular envelope cannot be controlled, because the actual location of the correlation peak can be anywhere in the window of the TIC.

As we have a good control on only two parameters of the detection process, namely, the period of the modulation (determined by the holographic beam splitter) and the phase of one of the RF input signals to the Bragg cells, we had to take into account these limitations in the design of the experimental verification of the performance of the data collection process.

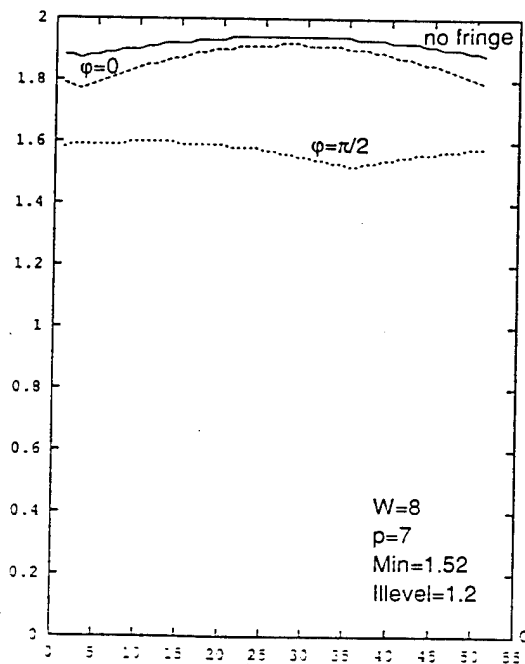
SIGNAL ON THE PIXEL  
COLLECTING THE MOST  
ENERGY



SIGNAL ON THE PIXEL  
COLLECTING THE MOST  
ENERGY



SIGNAL ON THE PIXEL  
COLLECTING THE MOST  
ENERGY



SIGNAL ON THE PIXEL  
COLLECTING THE MOST  
ENERGY

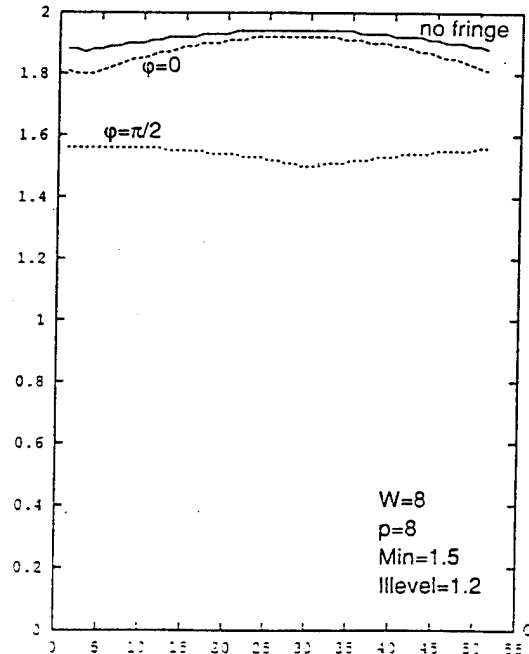
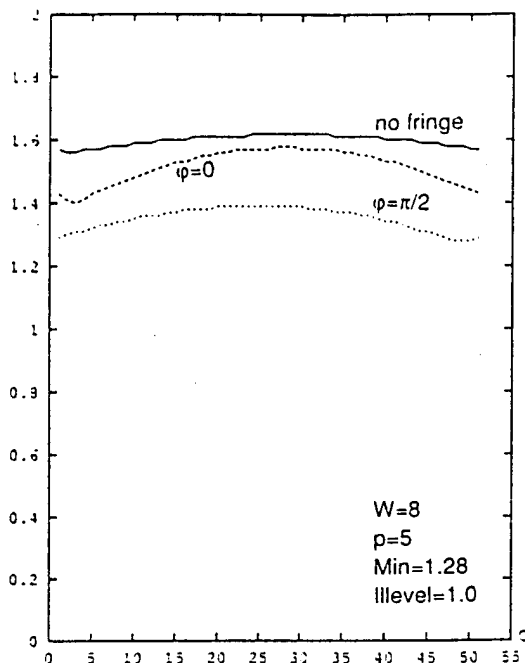
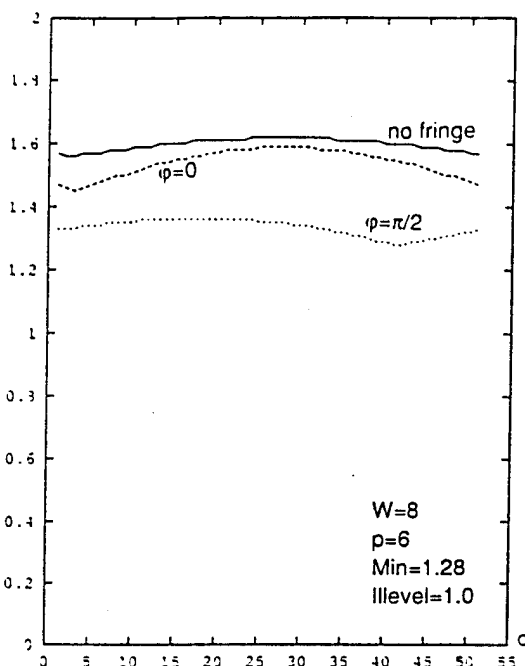


FIGURE 18: AMPLITUDE OF THE PEAK AS A FUNCTION OF THE POSITION OF THE APEX OF THE TRIANGULAR ENVELOPE ON THE DETECTING ELEMENT FOR  $W=6$  AND  $P=4, 5, 6$ , AND  $7$  FOR A RECTANGULAR SENSITIVITY RESPONSE

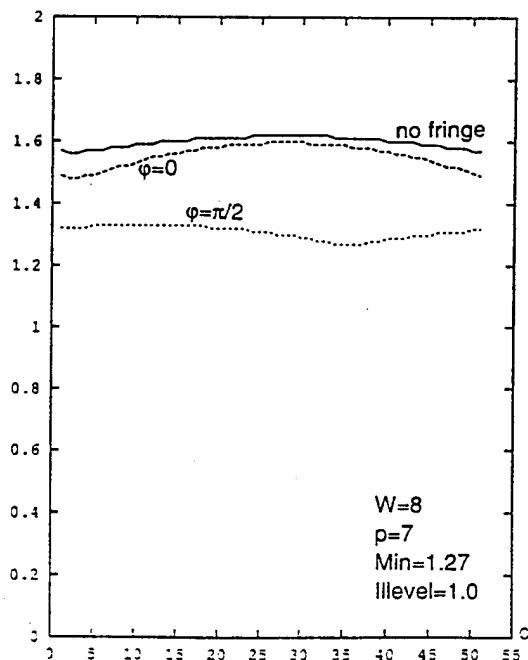
SIGNAL ON THE PIXEL  
COLLECTING THE MOST  
ENERGY



SIGNAL ON THE PIXEL  
COLLECTING THE MOST  
ENERGY



SIGNAL ON THE PIXEL  
COLLECTING THE MOST  
ENERGY



SIGNAL ON THE PIXEL  
COLLECTING THE MOST  
ENERGY

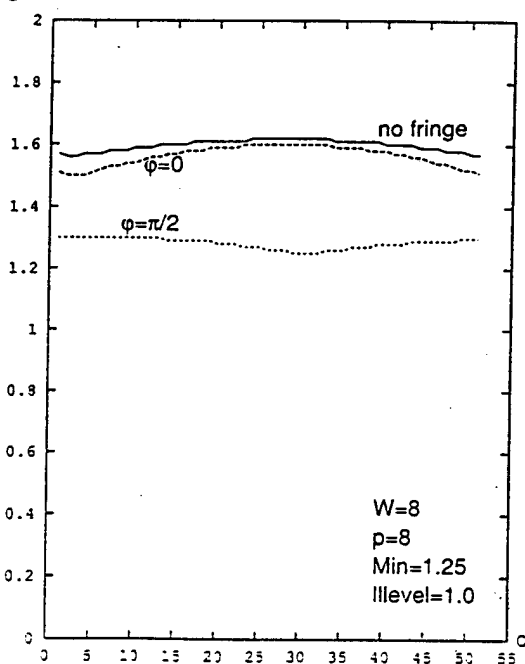


FIGURE 19: AMPLITUDE OF THE PEAK AS A FUNCTION OF THE POSITION OF THE APEX OF THE TRIANGULAR ENVELOPE ON THE DETECTING ELEMENT FOR  $W=6$  AND  $P=4, 5, 6$ , AND  $7$  FOR A THOMPSON CSF DETECTOR ARRAY WITH THE ILLUMINATION LEVEL INCREASED BY A FACTOR OF  $1.2$

Correlation Function

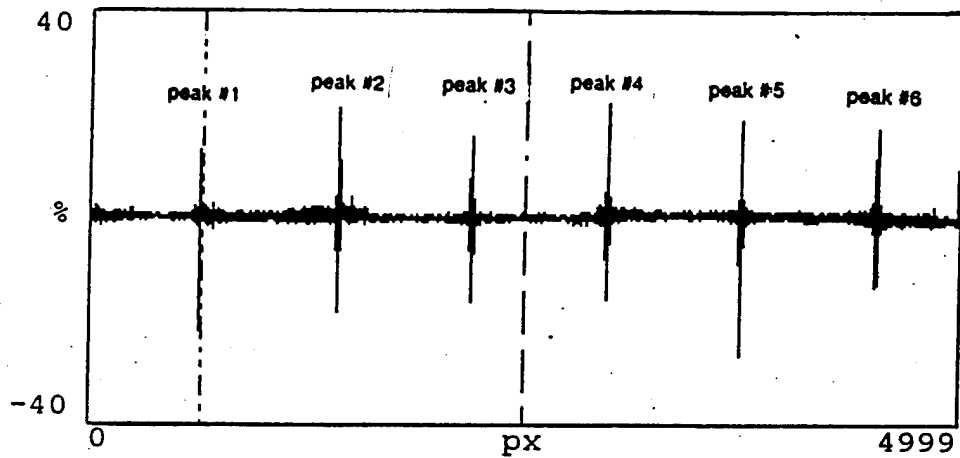


FIGURE 20: THE SIX AUTO CORRELATION PEAKS THAT APPEARS IN THE TIC WINDOW WHEN THE CHIP RATE IS 20 MHz

The optimal data collecting technique described in the previous paragraphs was tried on the autocorrelation of a pseudorandom sequence having 255 chips. At a chip rate of 20MHz, the duration of the sequence is 12.75  $\mu$ s and the 80  $\mu$ s window of the TIC will allow to observe 6 correlation peaks (Figure 20). The phase of the RF input to one of the Bragg cell was changed from 0 to 180° by increments of 10° and the amplitude of the correlation peak was observed for the six peaks. The results are illustrated in Figure 21. As expected from the results of the simulation, the amplitude of the peaks vary, but always stays within a detectable range. No blind spot is observed.

These results were confirmed by another experiment where a 7-chip long pseudorandom sequence was used. The chip rate was 10 MHz and a multitude of correlation peaks appear in the window (see Figure 22). Once again, variations of the amplitude of the peaks is observed, but all peaks are detectable, and no blind spot appears. The peak amplitude variations are commensurate with the results of the simulation for W=6 and P=5 where the peak amplitude was expected to vary between 1.45 and 1.9.

## 7.0 CONCLUSION

The features of the detection process of a TIC have been studied with a computer simulation and conditions of operation allowing a reliable detection of the correlation peaks over the whole operating window have been demonstrated experimentally. These conditions of operation have the further advantage to be associated with a graceful degradation of the performances of the detection process if the parameters drift away from their optimal value. Of particular importance is the fact that the detection process is not sensitive to large change of temperature when an optimal modulation is used. It was also demonstrated that the exact shape of the sensitivity response of the element of the detector array is a parameter of secondary importance in the evaluation of the performance of the detection process. Experimental verification of the optimal detection process has confirmed the capability to detect reliably correlation peaks over the whole field of view of the TIC.

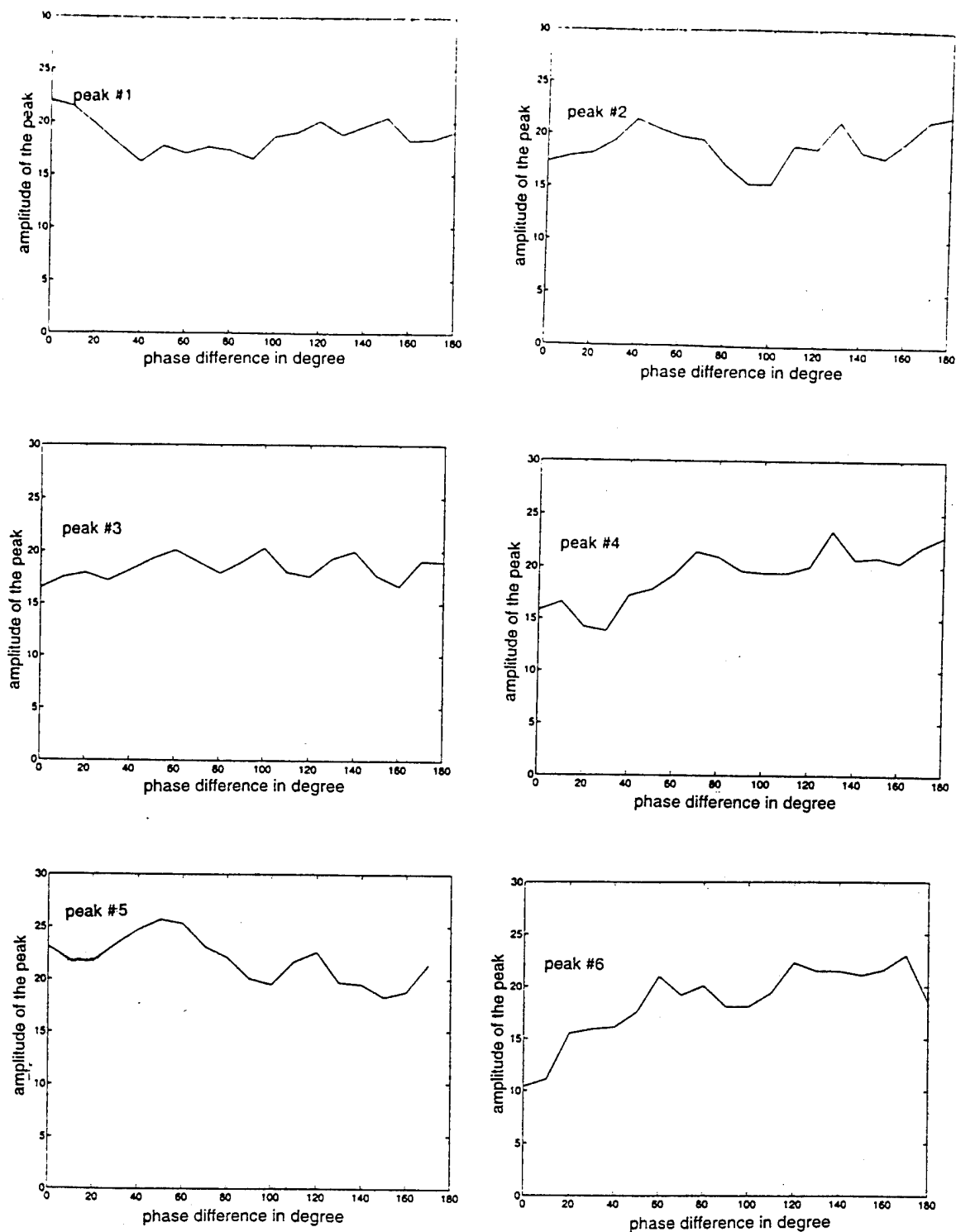


FIGURE 21: AMPLITUDE OF THE CORRELATION PEAKS OF FIGURE 20 AS A FUNCTION OF THE PHASE OF THE RF SIGNAL TO ONE BRAGG CELL



Correlation Function

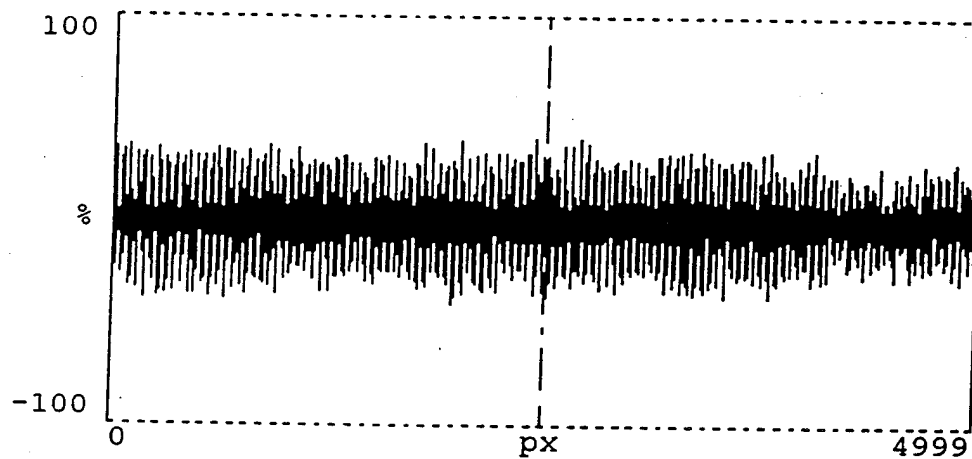


FIGURE 22: CORRELATION PEAKS PRODUCED BY A 7-CHIP LONG CODE  
WITH A CHIP RATE OF 10 MHz

## 8.0 REFERENCES

- [1] N. Brousseau, R. Brousseau, J.W.A. Salt, L. Gutz and M.D.B. Tucker, 'Analysis of DNA Sequences by an Optical Time-Integrating Correlator', Applied Optics, vol.31, no.23, 10 Aug. 1992, p. 4802-4815.
- [2] M.W. Casseday, N.J. Berg, I.J. Abramovitz and J.N. Lee, 'Wide-Band Signal processing Using the Two-Beam Surface Acoustic Wave Acoustooptic Time Integrating Correlator', IEEE Transactions on Sinics and Ultrasonics, vol. SU-28, no.3, May 1981, p. 205-212.
- [3] N.J. Berg and J.N. Lee, 'Acousto-Optic Signal Processing: Theory and Implementation', Marcel Dekker Inc., New York and Bassel, 1983, Chap.10.
- [4] P. Kelman, 'Time Integrating Optical Signal Processing', Ph.D. Dissertation, Dept. of Electrical Engineering, Stanford University, June 1979.
- [5] D.A.B. Fogg, 'A Compact Bulk Acousto-Optic Time-Integrating Correlator', Tech. Rep. ERL-0323-TR Department of Defence of Australia, Salisbury, Australia, 1984.
- [6] N. Brousseau and J.W.A. Salt, 'Two Compact Tandem Architecture for the Implementation of Time-Integrating Correlators', DREO TN 91-8.
- [7] A. Goutzoulis, D. Casasent and B.V.K. Kumar, 'Detector Effects on Time-Integrating Correlator Performance', Applied Optics, vol.24, no.8, 15 April 1985 p. 1224-1233.
- [8] N. Brousseau, 'Effects of Temperature Change on the Output of Time-Integrating Correlators', DREO TN 93-30.
- [9] C. Bélisle N. Brousseau and J.W.A. Salt, 'Evaluation Procedure for Linear Array Photosensitive Detector: Application to Thompson CSF TH 7805', DREO TN 89-6.

## APPENDIX A

### DECONVOLUTION OF THE MEASURED SENSITIVITY RESPONSE OF A DETECTOR ARRAY

The response of an element of the detector array is measured by scanning the element with a narrow light distribution while recording the energy collected by the element. The measured [9] response  $r(x)$  of the element of a detector array is thus the convolution of the light distribution  $i(x)$  used to perform the measurement with the sensitivity response  $s(x)$  of the detector element and we have

$$r(x) = i(x) * s(x) \quad (1)$$

where  $*$  indicates a convolution.  $r(x)$  and  $s(x)$  can be measured experimentally. The illumination pattern  $i(x)$  is produced by a diffraction limited cylindrical lens illuminated by a plane wavefront and focused on the element. As the detector is an energy sensitive device,  $i(x)$  can be written as

$$i(x) = [\sin(x)/x]^2 \quad (2)$$

The Fourier transform of equation 1 gives:

$$R(u) = I(u) \times S(u) \quad (3)$$

where  $R(u)$ ,  $I(u)$  and  $S(u)$  are respectively the Fourier transform of  $r(x)$ ,  $i(x)$  and  $s(x)$ . From equation 3, we can obtain:

$$S(u) = R(u) / I(u) \quad (3)$$

$$s(x) = F [R(u) / I(u)] \quad (4)$$

where  $F$  indicates the Fourier transform. However,

$$I(u) = F\{[\sin(x)/x]^2\} \quad (6)$$

$$= \{F[\sin(x)/x]\} * \{F[\sin(x)/x]\} \quad (7)$$

$$= \text{rect}(u) * \text{rect}(u) \quad (8)$$

$$= \text{triangle}(u) \quad (9)$$

So

$$s(x) = F[R(u)/\text{triangle}(u)] \quad (10)$$

The relative scaling of the illuminating function  $i(x)$  and of the measured sensitivity response  $r(x)$  was established (see Figure 21) from the width of the illumination pattern between its first null (3 mm) and the width of the detecting elements (13 mm). Equispaced samples were taken of these two functions.  $I(u)$  and the sensitivity response were calculated using equation 10 and a fast Fourier transform algorithm.

SECURITY CLASSIFICATION OF FORM  
(highest classification of Title, Abstract, Keywords)

**DOCUMENT CONTROL DATA**

(Security classification of title, body of abstract and indexing annotation must be entered when the overall document is classified)

1. ORIGINATOR (the name and address of the organization preparing the document. Organizations for whom the document was prepared, e.g. Establishment sponsoring a contractor's report, or tasking agency, are entered in section 8.) <b>DEFENCE RESEARCH ESTABLISHMENT OTTAWA</b> <b>NATIONAL DEFENCE</b> <b>SHIRLEYS BAY, OTTAWA, ONTARIO, K1A 0Z4 CANADA</b>		2. SECURITY CLASSIFICATION (overall security classification of the document including special warning terms if applicable)  <p align="center"><b>UNCLASSIFIED</b></p>	
3. TITLE (the complete document title as indicated on the title page. Its classification should be indicated by the appropriate abbreviation (S,C or U) in parentheses after the title.) <b>ANALYSIS AND OPTIMIZATION OF THE DATA COLLECTION PROCESS OF TIME-INTEGRATING CORRELATORS (U)</b>			
4. AUTHORS (Last name, first name, middle initial) <b>BROUSSEAU, N. AND SALT, J.W.A.</b>			
5. DATE OF PUBLICATION (month and year of publication of document)  <b>MARCH 1995</b>	6a. NO. OF PAGES (total containing information. Include Annexes, Appendices, etc.)  <p align="center"><b>48</b></p>	6b. NO. OF REFS (total cited in document)  <p align="center"><b>9</b></p>	
7. DESCRIPTIVE NOTES (the category of the document, e.g. technical report, technical note or memorandum. If appropriate, enter the type of report, e.g. interim, progress, summary, annual or final. Give the inclusive dates when a specific reporting period is covered.)  <b>DREO TECHNICAL NOTE</b>			
8. SPONSORING ACTIVITY (the name of the department project office or laboratory sponsoring the research and development. Include the address.) <b>DEFENCE RESEARCH ESTABLISHMENT OTTAWA</b> <b>NATIONAL DEFENCE</b> <b>SHIRLEYS BAY, OTTAWA, ONTARIO K1A 0Z4 CANADA</b>			
9a. PROJECT OR GRANT NO. (if appropriate, the applicable research and development project or grant number under which the document was written. Please specify whether project or grant)  <b>041LQ</b>	9b. CONTRACT NO. (if appropriate, the applicable number under which the document was written)		
10a. ORIGINATOR'S DOCUMENT NUMBER (the official document number by which the document is identified by the originating activity. This number must be unique to this document.)  <b>DREO TECHNICAL NOTE 95-5</b>	10b. OTHER DOCUMENT NOS. (Any other numbers which may be assigned this document either by the originator or by the sponsor)		
11. DOCUMENT AVAILABILITY (any limitations on further dissemination of the document, other than those imposed by security classification)  <input checked="" type="checkbox"/> Unlimited distribution <input type="checkbox"/> Distribution limited to defence departments and defence contractors; further distribution only as approved <input type="checkbox"/> Distribution limited to defence departments and Canadian defence contractors; further distribution only as approved <input type="checkbox"/> Distribution limited to government departments and agencies; further distribution only as approved <input type="checkbox"/> Distribution limited to defence departments; further distribution only as approved <input type="checkbox"/> Other (please specify):			
12. DOCUMENT ANNOUNCEMENT (any limitation to the bibliographic announcement of this document. This will normally correspond to the Document Availability (11). However, where further distribution (beyond the audience specified in 11) is possible, a wider announcement audience may be selected.)			

**UNCLASSIFIED**

SECURITY CLASSIFICATION OF FORM

13. ABSTRACT ( a brief and factual summary of the document. It may also appear elsewhere in the body of the document itself. It is highly desirable that the abstract of classified documents be unclassified. Each paragraph of the abstract shall begin with an indication of the security classification of the information in the paragraph (unless the document itself is unclassified) represented as (S), (C), or (U). It is not necessary to include here abstracts in both official languages unless the text is bilingual).

(U) The features of the detection process of a TIC have been studied with a computer simulation and optimal conditions of operation allowing a reliable detection of the correlation peaks over the whole operating window have been established. These optimal conditions of operation have the further advantage to be associated with a graceful degradation of the performances of the detection process if the parameters drift away from their optimal value. Of particular importance is the fact that the detection process is not sensitive to large change of temperature when an optimal fringe system is used. It was also demonstrated that the exact shape of the sensitivity response of the element of the detector array is a parameter of secondary importance in the evaluation of the performance of the detection process. Experimental verifications of the optimal detection process has confirmed their capability to detect reliably correlation peaks over the whole field of view of the TIC.

14. KEYWORDS, DESCRIPTORS or IDENTIFIERS (technically meaningful terms or short phrases that characterize a document and could be helpful in cataloguing the document. They should be selected so that no security classification is required. Identifiers, such as equipment model designation, trade name, military project code name, geographic location may also be included. If possible keywords should be selected from a published thesaurus. e.g. Thesaurus of Engineering and Scientific Terms (TEST) and that thesaurus-identified. If it is not possible to select indexing terms which are Unclassified, the classification of each should be indicated as with the title.)

TIME-INTEGRATING CORRELATORS  
DATA COLLECTION BY OPTICAL CORRELATORS  
OPTICAL CORRELATION  
OPTICAL CORRELATOR  
ANALOG CORRELATION  
ANALOG CORRELATOR